Master's thesis

NTNU
Norwegian University of Science and Technology
Faculty of Information Technology and Electrical Engineering
Department of Electronic Systems

Eirik Rokke

Cloud Radio Based Localization in Massive MIMO

Master's thesis in Electronics Systems Design and Innovation
Supervisor: Kimmo Kansanen
June 2019

NTNU
Kunnskap for en bedre verden

Eirik Rokke

Cloud Radio Based Localization in Massive MIMO

Master's thesis in Electronics Systems Design and Innovation
Supervisor: Kimmo Kansanen
June 2019

Norwegian University of Science and Technology
Faculty of Information Technology and Electrical Engineering
Department of Electronic Systems

NTNU
Norwegian University of
Science and Technology

Abstract

This project looks at the use of cloud radio-based localization in a massive MIMO. The system investigates a simple scenario, with plane waves, narrowband, no multipath and two spatially separated antenna arrays that are assumed to share information through cloud radio. Since a massive MIMO system is not phase aligned it was shown that it is necessary to have at least two transmitters and in this project, it was assumed that one of these was a beacon with a known position. When using two transmitters, an algorithm based on factor graphs for estimating the position of a transmitter was found. The found algorithm also produces an estimate of the error of its final estimate. In the simulations the algorithm gave good results and displayed the same behavior as the Cramer-Rao lower bound (CRLB) for a phase-aligned system, giving an estimate with an expected value of the true position. When increasing the received signal to noise ratio (SNR) from the beacon the error of the results also approach the CRLB. The estimated error gave results close to the true error when the received SNR from the beacon was 15-20 dB higher than the received SNR from the transmitter, and as long as both of the SNRs were over -2 dB.

Sammendrag

Dette prosjektet ser på bruken av cloud radio basert lokalisering i massiv MIMO. Systemet undersøker et simpelt scenario, med planbølger, narrowband, ingen flerveisinterferens og to romlig separerte antenne array som kan kommunisere via cloud radio. Siden det i massiv MIMO systemer ikke er fase samstilling er det vist at det er nødvendig med minst to sendere og i dette prosjektet er det antatt at en av disse er en beacon med kjent posisjon. Basert på faktor grafer ble det funnet en algoritme for å estimere posisjonen til en sender. Denne algoritmen produserer også et estimat på usikkerheten for posisjonsestimatet som den finner. Algoritmen gir gode resultater i simulasjoner og har samme oppførsel som CRLB for et system med fase samstilling, og algoritmen har den sanne posisjonen som forventningsverdi. Når SNRen til signalet fra beacon økes går også feilen i estimatet mot CRLB. Den estimerte usikkerheten gir også resultater som er nær den sanne feilen funnet under simuleringene så lenge SNRen til signalet fra beaconen var 15-20 dB høyere enn SNRen til signalet fra senderen, og så lenge begge SNRene var over -2 dB.

Contents

Chapter 1

Introduction

1.1 Problem description

In new communications systems, the use of massive MIMO has become more frequent. In these massive MIMO systems, cheap hardware is often used to reduce cost and to enable the use of the high number (>64) of antennas that are required at each site in such systems. The problem with cheap hardware is that the antennas are not phase-aligned but only phase-coherent (relative phase does not drift "quickly").

In new wireless networks, the localization of a transmitter is becoming more relevant [1]. Estimation of the angle of arrival (AoA) in MIMO can be done through many different estimation methods [2]. With the use of massive MIMO systems however, the estimation of localization through the AoA and distance can no longer be done using the phase estimates, as long as the systems are not phase-aligned. An estimate of the AoA can still be achieved using other methods that utilize the delay between received signals at each antenna. With the requirements of new systems, however, it is desirable to achieve better estimates than this. By using multiple spatially separated antenna arrays and exchange of information between these, it should be possible to get a better estimate of the AoA and from that the position.

1.2 Problem statement

This project will look at a system that uses two phase-coherent, but not phase aligned, massive MIMO antenna arrays and through collaboration estimates the position of a single transmitter. With this project, the aim is to find an algorithm for estimating the unknown position, as well as estimating the uncertainty of the estimated position. The performance of this algorithm will also be investigated in different scenarios, locations, SNR, etc. These scenarios will focus on finding problems that may occur because of spatial folding and the geometry of the antenna arrays.

1.3 Related work

The use of Massive MIMO in modern communication systems has increased in the last years and with 5G it is a leading technology [3]. In [4] they present the issues this will have for localization in such systems, and in [5] they present several topics regarding the future of Massive MIMO and in particular for localization. There is done some research on localization in Massive MIMO where [6] describes a method for doing direct localization on a distributed network in Massive MIMO. There is already done research on how to do distributed localization using several bearing estimates [7, 8, 9]. A single receiver is described in [10] which shows the effects of array structure, bandwidth and synchronization error. Within the field of MIMO radars, there is also done some work with distributed antennas, [11] shows concepts and applications in MIMO radars with widely separated antennas.

The use of factor graphs to describe algorithms was first done in [12], in [13] the factor graphs are explained more thoroughly. Pearl's Belief Propagation [14] is commonly used in factor graphs for message-passing and work with the sum-product algorithm described in [13]. To generalize and use these methods on different scenarios there has been done a lot of different work, in [15] the belief propagation was described in a purely gaussian scenario, which is described as Gaussian belief propagation (GaBF). Different approximations of message-passing have also been done, like in [16] which is based on the S-transform and in [17] which is a generalization of the different approximations based on the loopy belief propagation (GAMP).

In [18] cooperative localization is done with a factor graph using a combination of belief propagation and mean field message passing, and shows how to do localization in a distributed network.

Chapter 2

Theory

To solve the stated problem there is some important theory that is necessary to define. First, the signal model is described together with the receiver and transmitter design. Then some practical constraints are presented, with a focus on spatial folding and phase drift as well as some CRLB limits. After that estimators for direct estimation of the AoA are presented with a method for estimating the position from two AoA.

2.1 Signal model

Estimation of AoA and through that location is a well-known problem in array processing and this section describes theory related to this problem. First, the chosen receiver and transmitter design are stated. Then the received signal model both in continuous and discrete time, for the used system is presented. The received signal is also described for both a phase-coherent and a phase-aligned system.

2.1.1 Receiver and transmitter

The massive MIMO receiver used in this project is assumed to be an antenna array with a high number (>64) of antennas. The antenna array is assumed to be a uniform linear array (ULA) with a set element distance d_{rx}. The phase of the received signal is assumed to be dependant on the incident angle of the received signal, which will be described in Section 2.1.2.

In Figure 2.1 a block diagram of the proposed receiver is shown. Here each of the antennas is based on cheap hardware which would make the downmixer not phase-aligned between antennas, but still the same frequency. In the figure this is shown with the random phase ϕ_m that is present at each antenna, this is a random number between 0 and 2π. Each of the signals is sampled and they are combined in the digital signal processing. The signal is assumed to be oversampled and the matched filtering and downsampling is done digitally and the carrier frequency is noted as f_c. The signals $\boldsymbol{r}(t)$ and $\boldsymbol{r}[n]$ in Figure 2.1 are complex, so there is both and I and Q component coming from each of the antennas.

The transmitter is assumed to be a single antenna system that is transmitting a pseudo-random sequence of a set length that is assumed known at the receiver. In Figure 2.2, a block diagram of the transmitter is shown. The two signals $\boldsymbol{s}[n]$ and $\boldsymbol{s}(t)$ are complex oversampled signals in baseband, produced from the pseudo-random sequence.

2.1.2 Received signal

The transmitter is assumed to be in a not know position and transmitting a know pseudo-random sequence. We then use a complex baseband model to express the received signal at the antenna array $\boldsymbol{r}(t)$ and $\boldsymbol{r}[n]$ in figure 2.1, first in time domain and then the sampled discrete signal. The calculations and notations are influenced by the one used in chapter 7 of [19].

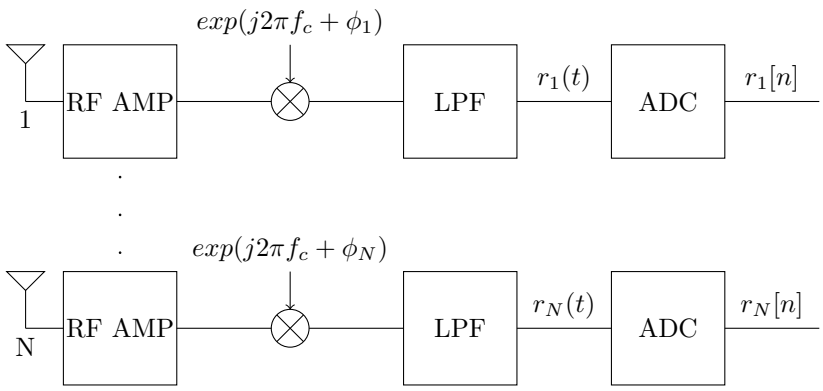

Figure 2.1: Receiver block diagram

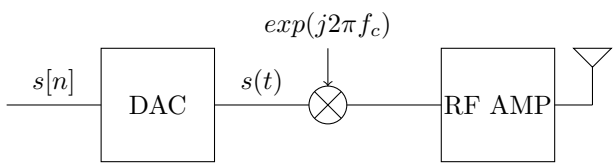

Figure 2.2: Transmitter block diagram

The receiver and transmitter are assumed to be fully synchronized, such that the receiver knows what signal it should receive at a certain time. Generally, antennas are not isotropic, this is however for simplicity not taken into account in the received signal model. The model will however still hold as long as the azimuth beam pattern is taken into account when describing the received SNR, which would make the SNR a function of angle. The received signal for a single antenna with this model is given as

$$r(t) = s(t) * g(t) * h(t) * f(t) + n(t).$$

Where $r(t)$ is the received signal, $s(t)$ the transmitted signal, $g(t)$ the transmit filter, $f(t)$ the receive filter, $h(t)$ the channel and $n(t)$ the noise. All of these are complex and $*$ denotes convolution. The noise is also assumed to be gaussian $n(t) \sim N(0, \sigma_n^2)$.

With an additive white Gaussian noise (AWGN) channel the channel gives an attenuation from the transmitter to the receiver, given by b. The channel also introduces a phase shift. Assuming correctly designed transmit and receive filter, the signal received at the antenna is given by the delayed transmitted signal, a phase rotation dependent on time and a random phase rotation introduced when the receiver is not phase aligned. With this, the received signal is then given as

$$r(t) = s(t - \tau) \cdot b \cdot \exp(j2\pi f_c \tau) \cdot \exp(j\phi) + n(t), \text{ for } \phi \sim U(0, 2\pi).$$

Where f_c is the carrier frequency and τ is the travel time between the transmitter and receiver. Substituting time with distance and speed this equation can also be written as

$$r(t) = s\Big(t - \frac{d}{c}\Big) \cdot b \cdot \exp\Big(j2\pi \frac{d}{\lambda}\Big) \cdot \exp(j\phi) + n(t).$$

Where λ is the wavelength of the carrier frequency, d is the distance between the transmitter and receiver and $b \cdot \exp\big(j2\pi \frac{d}{\lambda}\big) \cdot \exp(j\phi)$ can be seen as the channel $h(t)$.

With a receive antenna array as shown in Figure 2.3 with N number of antennas, antenna spacing d_{rx} and incident angle θ, the received signal at antenna m will then be given as

$$r_m(t) = s\Big(t - \frac{d_m}{c}\Big) \cdot b \cdot \exp\Big(j2\pi \frac{d_m}{\lambda}\Big) \cdot \exp(j\phi_m) + n(t).$$

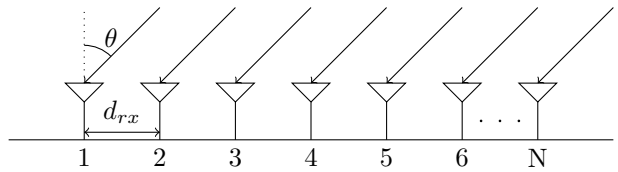

Figure 2.3: Antenna array

In the scenario with a single planewave from the transmitter to the receiver the delay at each antenna d_m is given by the distance between the transmitter and the receive antenna. This can also be expressed with the distance between the receiver and the first antenna and the incident angle of the planewave.

With a uniform linear array, ULA and 0° being broadside of the array, as in Figure 2.3. The distance to each antenna is given as

$$d_m = d_1 - \sin(\theta) \cdot d_{rx} \cdot (m-1), \text{ for } m = 1, ..., N.$$

Where d_1 is the distance to antenna one numbered from left to right, θ is the incident angle, d_{rx} is the distance between the antenna elements and m is the antenna number. The distances to each antenna can then be expressed in a vector format as

$$\boldsymbol{d} = [d_1 \ d_2 \ ... \ d_N]^T.$$

Where $\boldsymbol{d}$ is a column vector of the distances and $.^T$ denotes the transpose.

The channel for an antenna $h_m(t)$ can, in this case, be seen as the multiplication of two phase rotations and the attenuation b. The channel at each antenna is then given as

$$h_m(t) = b \cdot \exp\left(j2\pi\frac{d_m}{\lambda}\right) \cdot \exp(j\phi_m).$$

We can split the channel into three parts, first the attenuation b, then the phase rotation as a function of incident angle which we now refer to as $\boldsymbol{a}$ and lastly the random phase rotation caused by the receiver not being phase-aligned which we refer to as $\boldsymbol{e}$. The vectors $\boldsymbol{a}$ and $\boldsymbol{e}$ show the phase rotations over the antennas and can be expressed as

$$\boldsymbol{a} = [\exp\left(j2\pi\frac{d_1}{\lambda}\right) \ \exp\left(j2\pi\frac{d_2}{\lambda}\right) \ ... \ \exp\left(j2\pi\frac{d_N}{\lambda}\right)]^T \tag{2.1}$$

$$\boldsymbol{e} = [\exp(j\phi_1) \ \exp(j\phi_2) \ ... \ \exp(j\phi_N)]^T. \tag{2.2}$$

The channel at each antenna is then given by the elementwise multiplication between $\boldsymbol{a}$ and $\boldsymbol{e}$ and the attenuation as

$$h_m(t) = b \cdot a_m \cdot e_m \text{ for } m = 1, ..., N.$$

Which gives the channel vector as a function of the distance and as a function of the incident angle for all the antennas as

$$\boldsymbol{h}(\mathbf{d}) = b \cdot [\exp\left(j(2\pi\frac{d_1}{\lambda} + \phi_1)\right) \ \exp\left(j(2\pi\frac{d_2}{\lambda} + \phi_2)\right) \ ... \ \exp\left(j2\pi\frac{d_N}{\lambda} + \phi_N\right))]^T$$

$$\boldsymbol{h}(\boldsymbol{\theta}) = b \cdot [\exp\left(j(2\pi\frac{d_1}{\lambda} + \phi_1)\right) \ ... \ \exp\left(j(2\pi\frac{d_1 - \sin(\theta) \cdot d_{rx} \cdot N}{\lambda} + \phi_N)\right)]^T$$

$$\boldsymbol{h}(\boldsymbol{\theta}) = b \cdot \exp\left(j2\pi\frac{d_1}{\lambda}\right) \cdot [\exp(j\phi_1) \ ... \ \exp\left(j(-2\pi\frac{\sin(\theta) \cdot d_{rx} \cdot N}{\lambda} + \phi_N)\right)]^T. \tag{2.3}$$

Equation 2.3 show that the channel at each antenna is dependent on the random phase rotation ϕ_m and a phase rotation depending on the incident angle. It also show that a part depending on the distance to the first antenna d_1 can be moved out of the vector since it is present at all antennas.

The final received signal at each antenna for each time t is then given as

$$\boldsymbol{r}(t) = s\Big(t - \frac{d_m}{c}\Big) \cdot \boldsymbol{h}(\theta) + \boldsymbol{w}(t). \tag{2.4}$$

Where $\boldsymbol{w}(t)$ is a vector of the noise received at each antenna. The received signal is then given by the transmitted symbol, the channel expressed in Equation 2.3 and the noise.

With more than one antenna array, the received signal at each array would be given by $\boldsymbol{r}(t)$ with different values for d and depending on the array position relative to the other array and the transmitter.

For an equivalent discrete complex baseband system, the received signal will be given as

$$r[n] = s[n] * g[n] * h[n] * f[n] + w[n].$$

Where $r[n]$ is the received complex symbols, $s[n]$ the transmitted complex symbols, $g[n]$ the transmit filter, $f[t]$ the receive filter, $h[n]$ the channel and $w[n]$ the noise. All of these are complex. The noise is also assumed to be gaussian $n(t) \sim (0, \sigma_w^2)$.

Similar to the time domain signal an AWGN is used with attenuation equal to b. Since the system is not phase synchronized but sample synchronized there would be loss introduced in the sampling process within the main lobe of the correlation function. Here this loss is not taken into account, and will only lower the SNR of the received signal. With this, the channel only introduces a phase rotation. A random phase rotation will also be introduced by the receiver when it is not phase-aligned. The received signal is then given as

$$r[n] = s[n] \cdot \exp(j2\pi f_c \tau) \cdot \exp(j\phi) + w[n], \text{ for } \phi \sim U(0, 2\pi).$$

Where f_c is the carrier frequency and τ is the travel time between the transmitter and receiver. Substituting time with distance and speed this equation can also be written as

$$r[n] = s[n] \cdot \exp\left(j2\pi \frac{d}{\lambda}\right) \cdot \exp(j\phi) + w[n].$$

Where λ is the wavelength of the carrier frequency and d is the distance between the transmitter and receiver.

With a receive antenna array with N number of antennas the received signal at antenna m is then given by

$$r_m[n] = s(n) \cdot \exp\left(j2\pi \frac{d_m}{\lambda}\right) \cdot \exp(j\phi_m) + w[n].$$

Using the same scenario as for the continuous model, single planewave with $\boldsymbol{d}$ and $\boldsymbol{h}(\theta)$ given as before. The received signal can then be written using this as

$$\boldsymbol{r}[n] = s[n] \cdot \boldsymbol{h}(\theta) + \boldsymbol{w}[n]. \tag{2.5}$$

Here $\boldsymbol{h}$ can also be seen as the steering vector of the array, with the phase shift of the first antenna element not being one and including a random rotation at each antenna. Vector $\boldsymbol{w}[n]$ is the noise received at each antenna.

Given T number of received samples, the received signal matrix is given by

$$\boldsymbol{R} = \boldsymbol{h} \cdot \boldsymbol{s}^T + \boldsymbol{W}. \tag{2.6}$$

Where $\boldsymbol{R}$ is the received signal matrix, $\boldsymbol{h}(\theta)$ is the Nx1 channel vector, $\boldsymbol{s}$ is the Tx1 transmitted symbols vector from $n = 0$ to $n = T - 1$ and $\boldsymbol{W}$ is the NxT received noise matrix where each element is i.i.d. normal distributed.

Phase-coherent system

As in the signal model just described the received signal is not phase-aligned, but still, phase-coherent and the received signal will be given by Equation 2.5. To see how the random phase rotation alters the received signal it is interesting to look at the correlation matrix of the received signal,

$$R_{rr}(\theta) = \boldsymbol{h}\boldsymbol{h}^H + R_{nn}, \tag{2.7}$$

where $.^H$ denotes the Hermitian of the vector.

From this, it is not straightforward to see how the correlation matrix will behave, but using the definition of $\boldsymbol{h}$ in Equation 2.3 it is obvious that the diagonal will be a constant value b^2. The rest of the elements will be b^2 times a complex exponential. This complex exponential will have a phase given by the incident angle and the number of antennas between them and one random phase subtracted another. The two random phases can then be expressed as

$$\phi_{ij} = \phi_i - \phi_j.$$

Since each of the random phases have the same distribution $U(-\pi, \pi)$, the distribution of one subtracted another will, therefore, be the convolution between two equal uniform distributions, which then gives the probability distribution

$$P(\phi_{ij}) = P(\phi) * P(\phi) = \begin{cases} 1 - \frac{|\phi_{ij}|}{2\pi}, & |\phi_{ij}| \leq 2\pi \\ 0, & \text{otherwise} \end{cases}.$$

With the wrapping of phase at $\pm\pi$ this triangle distribution will end up becoming the same as that of one random phase $U(-\pi, \pi)$. The other phase component will just be a constant which does not change the distribution. The correlation matrix then ends up being b^2 on the diagonal and the rest are b^2 times a complex exponential with uniform random phase.

Given the distribution of each of the elements in the correlation matrix, it is clear that it would not be possible to estimate the incident angle from this. This is due to the wrapping of phases which end up causing each element of the matrix to be independent of the incident angle. If however the random phase vector $\boldsymbol{\phi}$ were known the correlation matrix would be dependant on the incident angle and could be used to estimate it.

Phase-aligned system

In this system, the antennas are not phase-aligned, but a similar phase-aligned system would work in almost an identical way. The received signal would be given as in Equation 2.5, but can be simplified since $\boldsymbol{e}$, which $\boldsymbol{h}$ depend on, would be all ones. Which would give the expression for the received signal as

$$\mathbf{r}[n] = s[n] \cdot \mathbf{h}(\theta) + \mathbf{w}[n] = s[n] \cdot b \cdot \mathbf{a} + \mathbf{w}[n]. \tag{2.8}$$

This scenario is an ideal case of the system that is not phase-aligned, if the random phase vector $\boldsymbol{\phi}$ in some way were perfectly estimated. Because of that, the limits of a phase-aligned system will also be the best case limits for the problem described here.

2.2 Practical constraints and limits

2.2.1 Spatial Folding

In most communication systems and other systems that do array processing with ULA, it is normal to use an antenna spacing that is no more than half of the wavelength. This is done to avoid spatial folding which is essentially causing multiple angles giving the same phase rotation. In massive MIMO systems, however,

it is possible that the distance is larger than half of the wavelength. With this spatial undersampling, one gets aliasing which can be described as spatial folding, and in AoA estimation this causes multiple angles to be equally likely being the correct one.

The only way to avoid or solve this issue is by having some prior information about the AoA that indicates which of these spatial folds corresponds to the true AoA. To get this prior information one must rely on methods that do not use phase information, one example of this is a correlation method which gives a difference in time of arrival at each antenna and therefore does not suffer from spatial folding problems.

2.2.2 Phase drifting

As mentioned previously the use of cheap hardware without phase-aligned downmixers in massive MIMO introduces some problems and for this project, in particular, the phase drifting and no phase-alignment are the most important. In [20] some of the hardware related problems at base stations are discussed. The use of cheap hardware introduces a random phase error at each antenna and since there is no synchronization this is a problem that has to be dealt with.

The phase drifting however is something that would be desirable to avoid dealing with directly in the estimation and it is, therefore, reasonable to look at how fast the phase would drift in a massive MIMO system. In [21] and [22] they describe the effects of phase noise and drifting, where both of them model the phase noise as a Wiener process such that the phase at each antenna m at sample n is given by

$$\phi_m[n] = \phi_m[n-1] + \omega_k[n]. \tag{2.9}$$

Where $\omega_k[n] \sim N(0, \sigma_\phi^2)$ which is independent at each antenna. Whereby definition $\sigma_\phi^2 = 4\pi^2 f_c^2 T_s c_\phi$, f_c is the carrier frequency, T_s is the symbol time and c_ϕ is dependant on the oscillator. As a typical value in a wireless system $c_\phi = 4.710^{-18}(\text{radHz})^{-1}$ and for this system the carrier frequency is assumed to be 900 MHz and the T_s is on the order of the inverse of the bandwidth which is assumed to be $0.1f_c$, which gives $\sigma_\phi^2 = 1.8555e-15$. This then gives the variance of the change in phase per symbol which in this case is really small and in the case of this project it can be neglected as long as the phase is reestimated often enough.

2.2.3 Limit of angle of arrival estimation

To get a limit on how good estimates one could hope to get, we look at the Cramer-Rao lower bound CRLB. The CRLB quantifies a lower bound on the variance one can achieve with an unbiased estimator for some parameter. First, we are looking at the CRLB for the estimated angle for a single antenna array that is phase-aligned, the CRLB for the position can be found from this. For simplicity we are doing these calculations on the real part of the signal, if assuming there is no correlation between the real and imaginary parts of the noise the CRLB for a complex signal will be half that of a real signal. The calculations are based on calculations and formulas given in [23]. Some of the calculation steps are skipped, but everything can be found in Appendix A.

For starting we have the received signal in a phase-aligned system as shown in Equation 2.8. Looking at a single snapshot of the received signal at a certain sample of n on then gets a value given as

$$\boldsymbol{r} = b \cdot \boldsymbol{a} \cdot s + \boldsymbol{w}.$$

Where $\boldsymbol{r}$, $\boldsymbol{a}$ and $\boldsymbol{w}$ is vectors going over the receiver antennas and b is the unknown attenuation.

Using only the real values one then gets an expression as

$$\boldsymbol{r} = C \cdot \cos(2\pi\psi m + \beta) + \boldsymbol{w}.$$

Where $\psi = -\frac{\sin(\theta)\cdot d_{rx}}{\lambda}$ is the spatial frequency for the change over the antennas, $\beta = 2\pi\frac{d_0}{\lambda}$ and $C = Real\{b\cdot s\}$. So here C, ψ and β are the unknowns which we put in the vector

$$\boldsymbol{\xi} = [C, \psi, \beta]^T. \tag{2.10}$$

With this we get the Fischer information matrix given by

$$\boldsymbol{I}(\boldsymbol{\xi}) = \frac{1}{\sigma_n^2} \begin{bmatrix} N/2 & 0 & 0 \\ 0 & 2C^2\pi^2(\frac{2N^3-3N^2+N}{6}) & C^2\pi\frac{(N-1)N}{2} \\ 0 & C^2\pi\frac{(N-1)N}{2} & \frac{NC^2}{2} \end{bmatrix}.$$

The CRLB for an estimate of θ with a complex signal is then given by

$$var(\hat{\theta}) \geq \frac{6}{(2\pi)^2 \cdot SNR \cdot N(N^2-1)} \frac{\lambda^2}{d_{rx}^2 \cos^2(\theta)}. \tag{2.11}$$

Where the signal to noise ratio SNR is given as

$$SNR = \frac{C^2}{2\sigma_n^2}. \tag{2.12}$$

This limit is assuming the use of one sample at each antenna. However, if more samples are used this can simply be expressed by increasing the SNR, assuming that these samples are coherently integrated. In Section 4.2 this CRLB will be used to get an indication of the limit when estimating the position with two antenna arrays.

2.3 Estimators

To estimate the position of a transmitter it would be desirable to estimate the AoA at two antenna arrays and use those two to estimate the position. In this chapter, a maximum likelihood (ML) estimator for the spatial frequency (which directly maps to the AoA) is presented and shown to be unusable when the system is not phase-aligned. Then a maximum a posteriori (MAP) estimator is presented and it is argued that it is necessary to first estimate the random phase and then estimate the position and two estimators for that is presented. Lastly, an approximation of the mapping from AoA to a position is presented when two antenna arrays are used.

2.3.1 Maximum likelihood estimator

For reference, it would be of interest to see what a ML estimator would give for a phase-aligned and a phase-coherent system. For simplicity and without any loss of generality we are going to consider the ML estimator for the spatial frequency $\psi = -2\pi\frac{\sin(\theta)d_{rx}}{\lambda}$ which is the phase rotation between each antenna. In this case, the ML estimator, as shown in example 7.17 in [19], will be given by

$$\underset{\hat{\psi}}{\operatorname{argmin}}\, I(\hat{\psi}) = \frac{1}{N}\sum_{m=1}^{N} |r_m \exp\Big(-j\hat{\psi}(m-1)\Big)|^2.$$

With r_m being the sampled received signal at antenna m at one time instance, for m going from 1 to N. Which given from Equation 2.5 for a single sample which gives

$$r_m = h_m s + w_m.$$

For a phase-aligned array this then simply gives the ML estimator

$$\underset{\hat{\psi}}{\operatorname{argmin}}\, I(\hat{\psi}) = \frac{1}{N}\sum_{m=1}^{N} |C\exp\left(j2\pi\frac{d_1}{\lambda}\right)\exp(j\psi(m-1))\exp\Big(-j\hat{\psi}(m-1)\Big) + w_m|^2.$$

It is easy to show the expected maximum of this is given when $\hat{\psi} = \psi$.

When the array is not phase-aligned the ML estimator is given by

$$\underset{\hat{\psi}}{\operatorname{argmin}}\, I(\hat{\psi}) = \frac{1}{N}\sum_{m=1}^{N} |C\exp\left(j2\pi\frac{d_1}{\lambda}\right)\exp(j\psi(m-1))\exp(j\phi_m)\exp\left(-j\hat{\psi}(m-1)\right) + w_m|^2.$$

With $\phi_m \sim U(-\pi,\pi)$ this will be given by

$$\underset{\hat{\psi}}{\operatorname{argmin}}\, I(\hat{\psi}) = \frac{1}{N}\sum_{m=1}^{N} |C\exp(j\phi'_m) + w_m|^2. \tag{2.13}$$

Where $\phi'_m \sim U(-\pi,\pi)$ is a shifted version of ϕ_m. Equation 2.13 show that the ML estimator, when the array is not phase-aligned, is independent of $\hat{\psi}$ and ψ, which indicate that this can not be used for estimating the spatial frequency or incident angle.

2.3.2 Maximum a posteriori estimation

As one could see in Section 2.3.1, it is not possible to do the estimation directly with an ML estimator. We are therefore looking at using MAP estimation for the spatial frequency ψ given a prior distribution of that spatial frequency. This is shown to also not be possible. An estimation of the random phases is found to be necessary and then there is also a need for two transmitters to avoid dependencies between the estimators. The estimation of the spatial frequency can then be done using the found estimate for the random phases and the prior for the spatial frequency. This way one transmitter is used to estimate the random phase and the other transmitters spatial frequency estimate is improved.

The estimation of the spatial frequency ψ is done instead of the estimation of the incident angle θ to simplify the calculations. There is a direct mapping between the two, so a correct estimate of one would give a correct estimate of the other. We are also assuming that we have a prior distribution for the spatial frequency, even though in reality we would get a prior for the position. Depending on the position the difference between these might be significant because of the sinusoid functions.

MAP for spatial frequency with prior for spatial frequency

Given a prior distribution of the spatial frequency ψ that is assumed to be given by $P(\psi)$. A MAP estimator for the incident angle given this prior would then be of interest. The received signal for a single sample will from Equation 2.5 then be given by

$$\boldsymbol{r} = s \cdot \boldsymbol{h}(\theta) + \boldsymbol{w}.$$

The incident angle and random phase will cause a phase shift at the received signal as expressed in Equation 2.3. The phase of the received signal is then expressed as

$$\boldsymbol{\alpha} = \angle(s \cdot \boldsymbol{h}(\theta)) = \angle s + 2\pi\frac{d_1}{\lambda} - 2\pi\frac{\sin(\theta)d_{rx}}{\lambda}(\boldsymbol{m}-1) + \boldsymbol{\phi},$$

where $\boldsymbol{m}$ is the antenna number as given before.

Without any loss of generality, the two constant phases that are common for all the antennas and that does not change with θ can be disregarded. The phase of the received signal at an antenna array can then be written as

$$\boldsymbol{\alpha} = -2\pi\frac{\sin(\theta)d_{rx}}{\lambda}(\boldsymbol{m}-1) + \boldsymbol{\phi}. \tag{2.14}$$

As explained previously we are looking at the estimation of the spatial frequency so we use $\psi = -2\pi\frac{\sin(\theta)d_{rx}}{\lambda}$ and the assumed prior $P(\psi_h)$ that we have for ψ_h, were ψ_h is used as the hypothesized spatial frequency to separate it from the true spatial frequency.

For a MAP estimation, we can then express the probability of getting the received signal by

$$P(\boldsymbol{r},\psi_h,\boldsymbol{\phi}_h) = P(\boldsymbol{r}|\psi_h,\boldsymbol{\phi}_h)P(\psi_h,\boldsymbol{\phi}_h) = P(\boldsymbol{r}|\psi_h,\boldsymbol{\phi}_h)P(\psi_h,\boldsymbol{\phi}_h) = P(\boldsymbol{r}|\psi_h,\boldsymbol{\phi}_h)P(\psi_h)P(\boldsymbol{\phi}_h).$$

Here the last equality holds since $\boldsymbol{\phi}_h$ and ψ_h are assumed independent.

The distribution of the received signal will then be given by

$$P(\boldsymbol{r}|\theta_h, \boldsymbol{\phi}_h) = \frac{1}{\pi^N|\Sigma|}\exp\big(-(\boldsymbol{r} - sb\exp(j\psi_h\boldsymbol{m} + \boldsymbol{\phi}_h))^H\Sigma^{-1}(\boldsymbol{r} - sb\exp(j\psi_h\boldsymbol{m} + \boldsymbol{\phi}_h))\big).$$

Here Σ is the covariance matrix of the noise at each antenna. Since the noise at each antenna is independent this can be simplified as

$$\begin{aligned}
P(\boldsymbol{r}|\psi_h, \boldsymbol{\phi}_h) &= \frac{1}{\pi^N N\sigma_w^2}\exp\left(-\frac{1}{\sigma_w^2}\sum_{m=1}^{N}(r_m - sb\exp(j\psi_h m + \phi_{h,m}))^*(r_m - sb\exp(j\psi_h m + \phi_{h,m}))\right)\\
P(\boldsymbol{r}|\psi_h, \boldsymbol{\phi}_h) &= \frac{1}{\pi^N N\sigma_w^2}\exp\left(-\frac{1}{\sigma_w^2}\sum_{m=1}^{N}|r_m|^2 - \frac{Ns^2b^2}{\sigma_w^2} + \frac{2}{\sigma_w^2}\sum_{m=1}^{N}|r_m|sb\cos(\psi m + \phi_{h,m} - \angle r_m)\right)\\
P(\boldsymbol{r}|\psi_h, \boldsymbol{\phi}_h) &= \frac{1}{\pi^N N\sigma_w^2}\exp\left(-\frac{1}{\sigma_w^2}\sum_{m=1}^{N}|r_m|^2\right)\exp\left(-\frac{Ns^2b^2}{\sigma_w^2}\right)\exp\left(\frac{2}{\sigma_w^2}\sum_{m=1}^{N}|r_m|sb\cos(\psi m + \phi_{h,m} - \angle r_m)\right)\\
P(\boldsymbol{r}|\psi_h, \boldsymbol{\phi}_h) &= \frac{1}{\pi^N N\sigma_w^2}\exp\left(-\frac{1}{\sigma_w^2}\sum_{m=1}^{N}|r_m|^2\right)\exp\left(-\frac{Ns^2b^2}{\sigma_w^2}\right)\prod_{m=1}^{N}\exp\left(\frac{2}{\sigma_w^2}|r_m|sb\cos(\psi m + \phi_{h,m} - \angle r_m)\right).
\end{aligned} \tag{2.15}$$

There is no prior information of $\boldsymbol{\phi}_h$ so this can take any value in its distribution $\phi_m \sim U(-\pi, \pi)$. So we have to integrate over $\boldsymbol{\phi}_h$ to get an estimator for ψ_h

The MAP estimator can then be expressed as

$$\hat{\psi}_{MAP} = \underset{\psi_h}{\operatorname{argmax}}\int_{-\pi}^{\pi} P(\boldsymbol{r}|\psi_h, \boldsymbol{\phi}_h)P(\psi_h)d\boldsymbol{\phi_h}.$$

The part not dependant on $\boldsymbol{\phi}$ can be moved out of the integral and the solution to the integral becomes

$$\begin{aligned}
\hat{\psi}_{MAP} = \underset{\psi_h}{\operatorname{argmax}}\, P(\psi_h)\frac{1}{\pi^N N\sigma_w^2}\exp\left(-\frac{1}{\sigma_w^2}\sum_{m=1}^{N}|r_m|^2\right)\exp\left(-\frac{Ns^2b^2}{\sigma_w^2}\right)\\
\int_{-\pi}^{\pi}\prod_{m=1}^{N}\exp\left(\frac{2}{\sigma_w^2}|r_m|sb\cos(\psi m + \phi_{h,m} - \angle r_m)\right)d\boldsymbol{\phi}_h
\end{aligned}$$

$$\begin{aligned}
\hat{\psi}_{MAP} = \underset{\psi_h}{\operatorname{argmax}}\, P(\psi_h)\frac{1}{\pi^N N\sigma_w^2}\exp\left(-\frac{1}{\sigma_w^2}\sum_{m=1}^{N}|r_m|^2\right)\exp\left(-\frac{Ns^2b^2}{\sigma_w^2}\right)\\
\prod_{m=1}^{N}\int_{-\pi}^{\pi}\exp\left(\frac{2}{\sigma_w^2}|r_m|sb\cos(\psi m + \phi_{h,m} - \angle r_m)\right)d\boldsymbol{\phi}_h.
\end{aligned}$$

Solving this integral then gives the solution

$$\hat{\psi}_{MAP} = \underset{\psi_h}{\operatorname{argmax}}\, P(\psi_h)\frac{1}{\pi^N N\sigma_w^2}\exp\left(-\frac{1}{\sigma_w^2}\sum_{m=1}^{N}|r_m|^2\right)\exp\left(-\frac{Ns^2b^2}{\sigma_w^2}\right)\prod_{m=1}^{N}2\pi I_0(\frac{|r_m|sb}{\sigma_w^2}),$$

where I_0 is the modified Bessel function of order zero.

By taking the logarithm and disregarding the parts that do not depend on θ_h this gives

$$\hat{\psi}_{MAP} = \underset{\psi_h}{\operatorname{argmin}}\ln(P(\psi_h)). \tag{2.16}$$

This shows that the first part of this estimate does not depend on ψ and therefore cannot be minimized over. The received signal r_m does depend on ψ, but this just shifts the uniform random phase ϕ_m which does not change the total phase distribution because of wrapping. This then means that without any prior knowledge about the random phase $\boldsymbol{\phi}$ the received signal gives no new information to estimate the spatial angular frequency ψ and from that the incident angle θ.

A possible solution to be able to improve the estimate of the spatial frequency ψ is introducing one additional transmitter. Then with a prior distribution of the incident angle for both of those, the random phase vector $\boldsymbol{\phi}$ is estimated using the signal from one of them and then that random phase estimate together with the prior for the incident angle is used to improve the estimate of the other incident angle.

To achieve this solution it is necessary to have an estimator for $\boldsymbol{\phi}$ given a prior for $\psi(\theta)$ and an estimator for ψ given a prior for both $\boldsymbol{\phi}$ and $\psi(\theta)$.

MAP for random phases with prior for spatial frequency

First, we are finding the MAP estimator for the random phase vector $\boldsymbol{\phi}$. In this case we only consider the case where the prior for the spatial frequency is uniform $U \sim (\mu_{\psi_h} - p, \mu_{\psi_h} + p)$. Using similar calculations as for the MAP estimator for ψ, a MAP estimator for $\boldsymbol{\phi}$ can then be found to be

$$\hat{\boldsymbol{\phi}}_{MAP} = \underset{\boldsymbol{\phi}_h}{\operatorname{argmax}} \int_{\mu_{\psi_h}-p}^{\mu_{\psi_h}+p} P(\boldsymbol{r}|\psi_h, \boldsymbol{\phi}_h) d\psi_h$$

$$\hat{\boldsymbol{\phi}}_{MAP} = \underset{\boldsymbol{\phi}_h}{\operatorname{argmax}} \frac{1}{\pi^N N \sigma_w^2} \exp\left(-\frac{1}{\sigma_w^2 \sum_{m=1}^N |r_m|^2}\right) \exp\left(-\frac{N s^2 b^2}{\sigma_w^2}\right)$$
$$\int_{\mu_{\psi_h}-p}^{\mu_{\psi_h}+p} \prod_{m=1}^N \exp\left(\frac{2}{\sigma_w^2}|r_m| \cos(\psi_h m + \phi_{h,m} - \angle r_m)\right) d\psi_h$$

$$\hat{\boldsymbol{\phi}}_{MAP} = \underset{\boldsymbol{\phi}_h}{\operatorname{argmax}} \int_{\mu_{\psi_h}-p}^{\mu_{\psi_h}+p} \prod_{m=1}^N \exp\left(\frac{2}{\sigma_w^2}|r_m| \cos(\psi_h m + \phi_{h,m} - \angle r_m)\right) d\psi_h. \tag{2.17}$$

This expression cannot be further simplified, but from the behavior of an exponential of a cosine, which gives maximum value with a value equal zero and since this function is symmetric and periodic with a period of 2π. This then gives that the maximum value is found when

$$\hat{\boldsymbol{\phi}}_{MAP} = \angle \boldsymbol{r} - \mu_{\psi_h} \boldsymbol{m}.$$

The distribution of this estimator is not easily identified, because the distribution of $\angle \boldsymbol{r}$ is complicated. There can however be done some approximations if one assumes that the noise power is small compared to that of the signal. The distribution of $\boldsymbol{r}$ can then be calculated, starting with the probability density function for the phase of a complex variable. Which gives the expression

$$P(\angle \boldsymbol{r}) = \frac{1}{\pi \sigma_w} \exp\left(-\frac{s^2 b^2}{\sigma_w^2} \sin^2(\angle \boldsymbol{r} - \boldsymbol{\alpha})\right)$$
$$[\frac{\sigma_w^2}{2} \exp\left(-\frac{s^2 b^2}{\sigma_w^2} \cos^2(\angle \boldsymbol{r} - \boldsymbol{\alpha})\right) + \frac{\sigma_w s b \cos(\angle \boldsymbol{r} - \boldsymbol{\alpha})\sqrt{\pi}}{2}[1 + \operatorname{erf}(\frac{sb}{\sigma_w} \cos(\angle \boldsymbol{r} - \boldsymbol{\alpha}))]]. \tag{2.18}$$

Where $\boldsymbol{\alpha}$ is the true phase of the received signal given by

$$\boldsymbol{\alpha} = \psi(\boldsymbol{m} - 1) + \boldsymbol{\phi}.$$

With the assumption that the noise power is much smaller than the signal power one can use that $sb >> \sigma_w$. From this one also gets $\sin(\angle \boldsymbol{r} - \boldsymbol{\alpha}) \approx \angle \boldsymbol{r} - \boldsymbol{\alpha}$ and $\cos(\angle \boldsymbol{r} - \boldsymbol{\alpha}) \approx 1$. The probability distribution in Equation 2.18 can be simplified to

$$P(\angle \boldsymbol{r}) = \frac{sb}{\sqrt{\pi}\sigma_w} \exp\left(-\frac{s^2b^2}{\sigma_w^2}(\angle \boldsymbol{r} - \boldsymbol{\alpha})^2\right)$$

$$P(\angle \boldsymbol{r}) = \frac{1}{\sqrt{2\pi \frac{\sigma_w^2}{s^2b^2}}} \exp\left(-\frac{(\angle \boldsymbol{r} - \boldsymbol{\alpha})^2}{2\frac{\sigma_w^2}{s^2b^2}}\right). \tag{2.19}$$

The last equation shows that with these assumptions the angle of the received signal is normally distributed with a variance of $\frac{\sigma_w^2}{s^2b^2}$ and mean of $\boldsymbol{\alpha}$ which is given by the true spatial frequency ψ and the true random phase vector $\boldsymbol{\phi}$. The distribution of the estimator is assumed uniform $U(\mu_{\psi_h} - p, \mu_{\psi_h} + p)$ which then gives a distribution for the estimator given by

$$P(\hat{\boldsymbol{\phi}}_{MAP}) = \frac{1}{(2b\sqrt{2\pi\sigma_w^2})} \int_{\boldsymbol{\alpha}+(\mu_{\psi_h}-p)(\boldsymbol{m}-1)}^{\boldsymbol{\alpha}-(\mu_{\psi_h}+p)(\boldsymbol{m}-1)} \exp\left(-\frac{(\tau - \hat{\boldsymbol{\phi}}_{MAP})^2}{2\sigma_w^2}\right) d\tau. \tag{2.20}$$

Since the limits of the integral are dependant on the antenna number $\boldsymbol{m}$, this distribution will become "flatter" as m increases. The fact that the phases would wrap at $\pm\pi$ is not taken into account here, but this still gives an indication of how the estimator will behave.

In the scenario where the position of the transmitter is known perfectly, the integral is no longer needed and one ends up with

$$P(\hat{\boldsymbol{\phi}}_{MAP}) = \frac{1}{\sqrt{2\pi \frac{\sigma_w^2}{s^2b^2}}} \exp\left(-\frac{(\hat{\boldsymbol{\phi}}_{MAP} - \psi(\boldsymbol{m}-1))^2}{2\frac{\sigma_w^2}{s^2b^2}}\right). \tag{2.21}$$

The distribution of the estimator is then gaussian with a mean of $\boldsymbol{\phi}$ and variance of $\frac{\sigma_w^2}{s^2b^2}$.

With these different posteriori distributions it is clear that as long as the prior distribution for ψ is sufficiently good, meaning that $N-1$ times the maximum error does not exceed π such that the distribution starts wrapping around, one gets an estimator for $\boldsymbol{\phi}$ with the true value as the expected value. If the maximum error exceeds π for some of the antennas, there cannot be given any new estimates for these and they will not give any additional information when estimating the spatial frequency. On the other hand, if the position is known perfectly, the estimate for $\boldsymbol{\phi}$ will be Gaussian distributed with a variance that depends inversely on the signal to noise ratio. This case is reasonable, for example, if one uses the other antenna array as the transmitter used for estimating $\boldsymbol{\phi}$, then one would know the position perfectly.

MAP for spatial frequency with prior for random phase and spatial frequency

To do the estimation for ψ a given prior for both ψ and $\boldsymbol{\phi}$ is required. The estimator will be the same as the estimator for ψ without the prior for $\boldsymbol{\phi}$ except the limits of the integral will be changed. Here one would ideally use the posteriori found from the previous estimator as a prior, but this complicates the calculations and instead, we are assuming that the prior we have for $\boldsymbol{\phi}$ is a uniform distribution with mean equal zero and limits $\pm\sigma_{\phi_h}$. The mean of zero can easily be achieved by just rotating the received signal by negative the mean of any uniform distribution. By assuming that the prior is uniform some of the information from the found posteriori will be lost, but the narrower the posteriori becomes this assumption becomes more accurate. This gives the MAP estimator given as

$$\hat{\psi}_{MAP} = \underset{\psi_h}{\operatorname{argmax}}\, P(\boldsymbol{r}|\psi_h, \boldsymbol{\phi}_h)P(\psi_h)P(\boldsymbol{\phi}_h)$$

$$\hat{\psi}_{MAP} = \underset{\psi_h}{\operatorname{argmax}}\, P(\psi_h) \prod_{m=1}^{N} \int_{-\sigma_{\phi_h}}^{\sigma_{\phi_h}} \exp\left(\frac{2}{\sigma_w^2}|r_m| sb\cos(\psi_h(m-1) + \phi_{h,m} - \angle r_m)\right) d\boldsymbol{\phi}_h.$$

The integral in this expression is not directly solvable, but a Taylor series expansion can be done. The third order expansion is given by

$$\hat{\psi}_{MAP} = \underset{\psi_h}{\operatorname{argmax}}\, P(\psi_h) \prod_{m=1}^{N} \int_{-\sigma_{\phi_h}}^{\sigma_{\phi_h}} \exp\left(\frac{2|r_m|sb}{\sigma_w^2}\right) - \frac{1}{2}\frac{2|r_m|sb}{\sigma_w^2}\exp\left(\frac{2|r_m|sb}{\sigma_w^2}\right)(\psi_h(m-1)+\phi_{h,m}-\angle r_m)^2 + \frac{1}{24}\frac{2|r_m|sb}{\sigma_w^2}(3\frac{2|r_m|sb}{\sigma_w^2}+1)\exp\left(\frac{2|r_m|sb}{\sigma_w^2}\right)(\psi_h(m-1)+\phi_{h,m}-\angle r_m)^4 d\boldsymbol{\phi}_h.$$

This integral can be solved and by taking the logarithm one gets a sum instead of a product. The expression for the MAP estimator is then given as

$$\begin{aligned}\hat{\psi}_{MAP} = \underset{\psi_h}{\operatorname{argmax}}\, P(\psi_h) \sum_{m=1}^{N} \ln\Big[&\exp\left(\frac{2|r_m|sb}{\sigma_w^2}\right)((\psi_h(m-1)+\sigma_{\phi_h}-\angle r_m)-(\psi_h(m-1)-\sigma_{\phi_h}-\angle r_m)) \\ &-\frac{1}{6}\frac{2|r_m|sb}{\sigma_w^2}\exp\left(\frac{2|r_m|sb}{\sigma_w^2}\right)((\psi_h(m-1)+\sigma_{\phi_h}-\angle r_m)^3-(\psi_h(m-1)-\sigma_{\phi_h}-\angle r_m)^3) \\ &+\frac{1}{120}\frac{2|r_m|sb}{\sigma_w^2}(3\frac{2|r_m|sb}{\sigma_w^2}+1)\exp\left(\frac{2|r_m|sb}{\sigma_w^2}\right)((\psi_h(m-1)+\sigma_{\phi_h}-\angle r_m)^5-(\psi_h(m-1)-\sigma_{\phi_h}-\angle r_m)^5\Big].\end{aligned} \tag{2.22}$$

From Equation 2.22 it is not easy to see what results this would give. It is, however, an equation that would give the estimated value and it requires fewer computations than the one including an integral in Equation 2.3.2, which would be simpler to calculate numerically. The reason the value $\psi_h(m-1)-\sigma_{\phi_h}-\angle r_m$ is kept as is and not simplified is because this total phase needs to be wrapped down to achieve a correct result since the original function wrapped around at 2π and the Taylor expansion only holds for small values.

Combining the two MAP estimators for $\boldsymbol{\phi}$ and ψ with two transmitters will then probably produce a better estimate for one of the transmitters, assuming the prior for the ψ used to estimate $\boldsymbol{\phi}$ is good enough. To achieve this one could use the other antenna array as one of the transmitters, and that way one has perfect knowledge of ψ.

2.3.3 Linear approximation for triangulation

There are a lot of ways to get from angles to positions using triangulation. In the scenario described here however we are only considering the case of two angles to get a position.

Using simple triangulation in a system when one assumes that both of the y-positions for the known positions are zero one can show that the position is given by

$$p_x = \frac{x_1\tan(\alpha)+x_2\tan(\beta)}{\tan(\alpha)+tan(\beta)} \tag{2.23}$$

$$p_y = \frac{(x_2-x_1)\tan(\alpha)\tan(\beta)}{\tan(\alpha)+tan(\beta)}. \tag{2.24}$$

Where α and β are the angles given by the angle between incoming wave and the x-axis as shown in figure 2.4.

The two equations for the position are not too complicated, but they both depend on both of the angles and they are not linear. As described in Section 3.1 about factor graphs it is desirable to have linear function nodes. There is therefore interesting to see if it is possible to do find a good linear estimate of these two functions. This can be done by using both of the functions in a vector Taylor expansion, where the function is given by

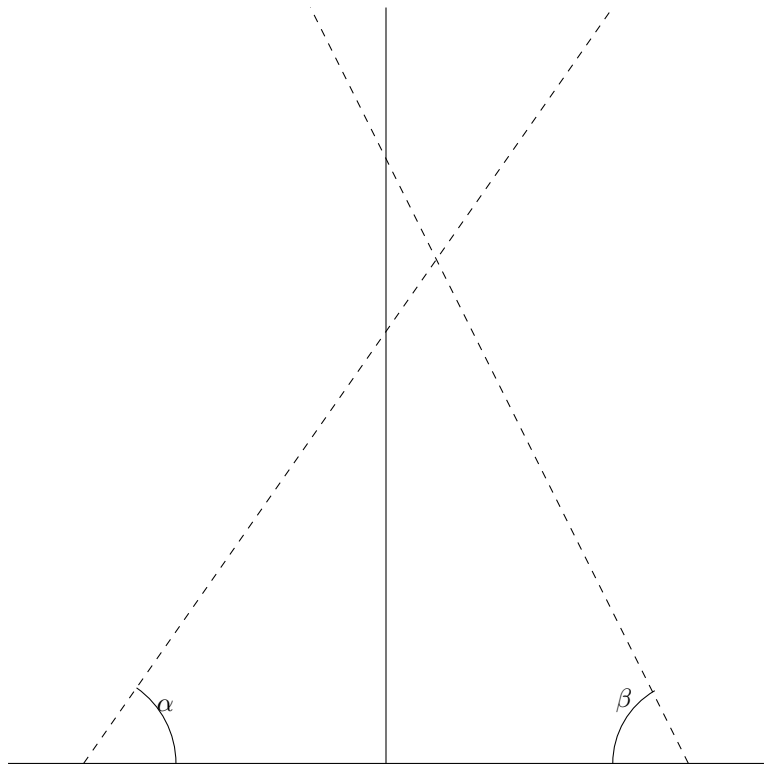

Figure 2.4: Triangulating

$$\boldsymbol{p}(\alpha, \beta) = [p_x(\alpha, \beta), p_y(\alpha.\beta)]^T.$$

In the factor graphs, when doing a gaussian belief propagation GaBF which is described later, the means and variances are all the information propagating between the nodes. It is, therefore, reasonable to do the Taylor expansion around these means. The Taylor expansion can then be given as

$$\hat{\boldsymbol{p}}(\alpha, \beta) = \begin{bmatrix} p_x(\mu_\alpha, \mu_\beta) \\ p_y(\mu_\alpha.\mu_\beta) \end{bmatrix} + \begin{bmatrix} \frac{\partial p_x}{\partial \alpha}(\mu_\alpha, \mu_\beta) & \frac{\partial p_x}{\partial \beta}(\mu_\alpha, \mu_\beta) \\ \frac{\partial p_y}{\partial \alpha}(\mu_\alpha, \mu_\beta) & \frac{\partial p_y}{\partial \beta}(\mu_\alpha, \mu_\beta) \end{bmatrix} \begin{bmatrix} \alpha - \mu_\alpha \\ \beta - \mu_\beta \end{bmatrix}.$$

The derivatives needed can be calculated and they are expressed as

$$\frac{\partial p_x}{\partial \alpha} = \frac{(x_1 - x_2)\frac{\tan(\beta)}{\cos^2(\alpha)}}{(\tan(\alpha) + tan(\beta))^2}$$

$$\frac{\partial p_x}{\partial \beta} = \frac{(x_2 - x_1)\frac{\tan(\alpha)}{\cos^2(\beta)}}{(\tan(\alpha) + tan(\beta))^2}$$

$$\frac{\partial p_y}{\partial \alpha} = \frac{(x_2 - x_1)\frac{\tan^2(\beta)}{\cos^2(\alpha)}}{(\tan(\alpha) + tan(\beta))^2}$$

$$\frac{\partial p_y}{\partial \beta} = \frac{(x_2 - x_1)\frac{\tan^2(\alpha)}{\cos^2(\beta)}}{(\tan(\alpha) + tan(\beta))^2}.$$

With this one can find the Taylor expansion for each of the functions which are then given by

$$\hat{p}_x = p_x(\mu_\alpha, \mu_\beta) + (\alpha - \mu_\alpha)\frac{\partial p_x}{\partial \alpha}(\mu_\alpha, \mu_\beta) + (\beta - \mu_\beta)\frac{\partial p_x}{\partial \beta}(\mu_\alpha, \mu_\beta) \tag{2.25}$$

$$\hat{p}_y = p_y(\mu_\alpha, \mu_\beta) + (\alpha - \mu_\alpha)\frac{\partial p_y}{\partial \alpha}(\mu_\alpha, \mu_\beta) + (\beta - \mu_\beta)\frac{\partial p_y}{\partial \beta}(\mu_\alpha, \mu_\beta). \tag{2.26}$$

Equation 2.25 and 2.26 can then be used to calculate the means and as long as the true value is not "too far" from the estimated means (the variance is low) this is a good approximation. Since it also is of interest to get the variances in the case of the factor graphs we can in this case look at the covariance matrix

$$\Sigma_p = Cov(\hat{\boldsymbol{p}}) = E[\hat{\boldsymbol{p}}\hat{\boldsymbol{p}}^T] - E[\hat{\boldsymbol{p}}]E[\hat{\boldsymbol{p}}]^T.$$

This can be solved and using that the expected value of $(\alpha - \mu_\alpha)$ and $(\beta - \mu_\beta)$ is zero, where the arguments μ_α and μ_β are excluded for notation purposes, this ends up being

$$\Sigma_p = \begin{bmatrix} (\frac{\partial p_x}{\partial \alpha})^2 Var(\alpha) + (\frac{\partial p_x}{\partial \beta})^2 Var(\beta) & \frac{\partial p_x}{\partial \alpha}\frac{\partial p_y}{\partial \alpha} Var(\alpha) + \frac{\partial p_x}{\partial \beta}\frac{\partial p_y}{\partial \beta} Var(\beta) \\ \frac{\partial p_x}{\partial \alpha}\frac{\partial p_y}{\partial \alpha} Var(\alpha) + \frac{\partial p_x}{\partial \beta}\frac{\partial p_y}{\partial \beta} Var(\beta) & (\frac{\partial p_y}{\partial \alpha})^2 Var(\alpha) + (\frac{\partial p_y}{\partial \beta})^2 Var(\beta) \end{bmatrix}.$$

From this one can find the variance and covariance of the two individual functions and their covariance given by

$$\sigma^2_{p_x} = (\frac{\partial p_x}{\partial \alpha}(\mu_\alpha, \mu_\beta))^2 \sigma^2_{\theta_1} + (\frac{\partial p_x}{\partial \beta}(\mu_\alpha, \mu_\beta))^2 \sigma^2_{\theta_2} \tag{2.27}$$

$$\sigma^2_{p_y} = (\frac{\partial p_y}{\partial \alpha}(\mu_\alpha, \mu_\beta))^2 \sigma^2_{\theta_1} + (\frac{\partial p_y}{\partial \beta}(\mu_\alpha, \mu_\beta))^2 \sigma^2_{\theta_2} \tag{2.28}$$

$$Cov(p_x, p_y) = (\frac{\partial p_x}{\partial \alpha}(\mu_\alpha, \mu_\beta))(\frac{\partial p_y}{\partial \alpha}(\mu_\alpha, \mu_\beta)) Var(\alpha) + (\frac{\partial p_x}{\partial \beta}(\mu_\alpha, \mu_\beta))(\frac{\partial p_y}{\partial \beta}(\mu_\alpha, \mu_\beta)) Var(\beta). \tag{2.29}$$

The mean of the position can then be found using Equation 2.23 and 2.24 and one simply gets

$$\mu_{p_x} = p_x(\mu_\alpha, \mu_\beta)$$

$$\mu_{p_y} = p_y(\mu_\alpha, \mu_\beta).$$

The error in this approximation is difficult to predict, as it is dependent on the variance and mean of both of the angle estimates. The error would, however, be given by the second derivative and would give a tensor notation.

Chapter 3

Method

As described in Chapter 2, it is possible to use MAP estimators to estimate the AoA at each antenna array, and it is also necessary to have two transmitters for the estimation. Instead of using the MAP estimators and find a position it is desirable to have a complete estimation process that is simpler. The final system is therefore based on factor graphs, which should achieve the same performance with simpler calculations. Factor graphs are a method of describing algorithms, and an introduction to factor graph is given in Section 3.1. After that, the estimation of the position is represented using two factor graphs, one to estimate the random phase and the other to estimate the position.

3.1 Factor graphs introduction

Factor graphs are a way to describe algorithms and how they function in a simple as possible manner. In [13] factor graphs and the sum-product algorithm is explained in detail. What follows will be a simple explanation with a focus on the parts of most interest in this project and to explain notation that will be used later.

A factor graph is essentially a factorization of a function into smaller parts, and this can be displayed graphically. These factor graphs are then build up of function nodes, variable nodes, and edges which connect the nodes. The variable nodes represent a visible (measured) or hidden variable that is connected through one or more edges with function node(s). The function node then represents a local function that has some variables it depends on.

In Figure 3.1 a simple factor graph is displayed. This factor graph represent the function $y = x + m + n$, where y is an observed variable, x is the variable we want to estimate, m hidden unknown interference with a prior given by f_m and n the hidden unknown additive noise given by the prior f_n. To get an estimate for x one needs to calculate the messages going at each edge. Notation for these messages vary in the literature, here we use the notation $\mu_{f_m - m}(m)$ and $\mu_{m - f_m}(m)$ for messages passing from and to function nodes respectively. These messages then need to be calculated and here this is done using belief propagation with the sum-product algorithm. Which gives the two functions for calculating a message to and from a function node as

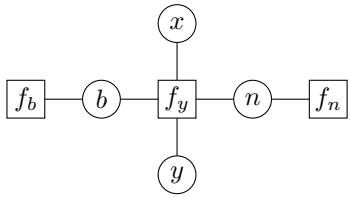

Figure 3.1: Factor graph example

$$\mu_{z_i - f_z}(z_i) = \prod_{j=1}^{M} \mu_{f_j - z_i}(z_i)) \tag{3.1}$$

$$\mu_{f_z - z_i}(z_i) = \int_{\sim z_i} (f_z(\boldsymbol{z}) \prod_{j=1}^{N} \mu_{z_j - f_z}(z_j)) d \sim z_i, \tag{3.2}$$

where z_i is some variable and f_z is a function. (Where the notation $\sim z_i$ means all the values of $\boldsymbol{z}$ except z_i)

Here Equation 3.1 expresses that a message from a variable node to a function node is given by the product of the message from all other function nodes to that variable. And Equation 3.2 that the message from a function node to a variable node is the integral, over all the other variables connected to that function, of the function itself times the product of the messages from all other variables.

To calculate these messages one would, therefore, need to start at the nodes at the end, which have only one connection and then work inwards/upwards from there. For example in the factor graph in Figure 3.1 when y is measured and x is unknown first the messages $\mu_{f_m - m}(m)$, $\mu_{f_n - n}(n)$ and $\mu_{y - f_y}(y)$ must be calculated, then $\mu_{m - f_y}(m)$ and $\mu_{n - f_y}(n)$ and lastly the message $\mu_{f_y - x}(x)$. In the end, the marginal distribution for a variable can be found by multiplying all the incoming messages, since there, in this case, is no prior for x the distribution for x would then simply be given by the incoming message from f_y.

Using Equation 3.1 and 3.2 one can calculate the mentioned messages needed in Figure 3.1, the last message $\mu_{f_y - x}(x)$ to x would then be given as

$$\mu_{f_y - x}(x) = \int_m \int_n (\delta(x + m + n - y) f_m(m) f_n(n)) dn dm. \tag{3.3}$$

Solving Equation 3.3 would then give the distribution of the variable of interest x. Doing this integral is computationally heavy and it is desirable to avoid, if possible. In hardware, this would be done by using a discrete estimation, but this is also something that is desirable to avoid because of the errors it introduced. In larger problems where lots of these integrals would need solving it is, therefore, necessary to do some approximations. A good approximation of this problem could be done using GAMP [17]. However, in the factor graph used in this project, which is described later, it is assumed that all the underlying distributions are Gaussian and that all the functions are linear. This simplifies the calculations significantly and GAMP is no longer necessary and one ends up using the less general gaussian belief propagation (GaBF)[15]. With GaBF the messages then end up just being means and variances (covariance matrix). With this approximation, one does, however, limit all the function nodes to being linear, which is not normally the case. Simple first order Taylor expansion is ,therefore, a good approximation as long as the variance is not too big.

In the case of Figure 3.1 using GaBF, all the messages then end up being given as

$$\boldsymbol{\eta}_{f_m - m}(m) = [\mu_m, \sigma_m^2]^T$$
$$\boldsymbol{\eta}_{m - f_y}(m) = [\mu_m, \sigma_m^2]^T$$
$$\boldsymbol{\eta}_{f_n - n}(n) = [\mu_n, \sigma_n^2]^T$$
$$\boldsymbol{\eta}_{n - f_y}(n) = [\mu_n, \sigma_n^2]^T$$
$$\boldsymbol{\eta}_{y - f_y}(y) = y$$

$$\boldsymbol{\eta}_{f_y - x}(m) = [y - \mu_m - \mu_n, \sigma_m^2 + \sigma_n^2]^T$$
$$\boldsymbol{\eta}_{f_y - x}(m) = [\mu_x, \sigma_x^2]^T.$$

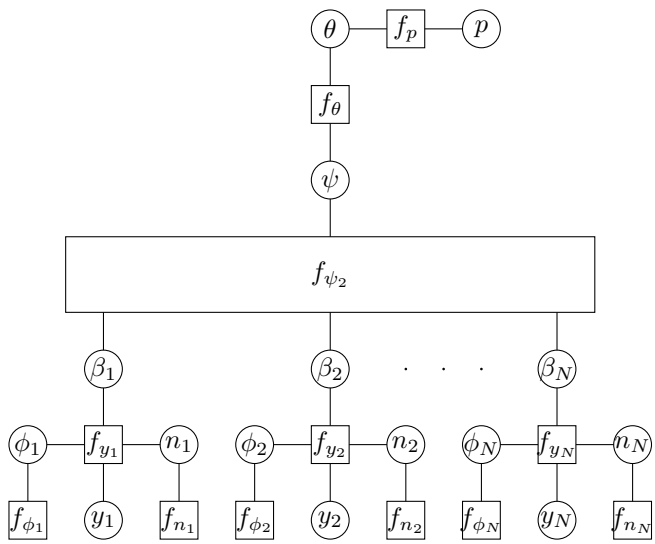

Figure 3.2: Factor graph, synchronization, antenna array

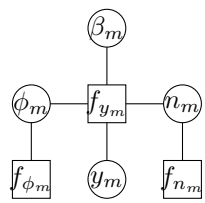

Figure 3.3: Factor graph, synchronization, single antenna

$\boldsymbol{\eta}$ is used as the message sent on edges in GaBF, being a vector of the means and variances. With the last two equations giving the calculations done in node f_y, and also giving the variables needed to precisely know the distribution of x. Which, in the simple example given here, it is easy to see that this result is correct, and could have been calculated in a much simpler way, however, when the graph is bigger this is no longer a simple solution.

All of the above examples, however, are done with the assumption that the total function can be factorized without dependencies. If this can not be done you end up with a factor graph which includes "loops", which makes the standard message-passing impossible. In the case of loops, one has to resort to the loopy belief propagation, which is similar to the standard belief propagation by just assuming that the messages that have not been calculated yet are equal to one. Because of this one needs to iterate the calculations of each message and the convergence of the result is difficult to predict. When doing GaBF however it is shown in [15] that it does converge.

3.2 Factor graph for beacon

In Figure 3.2 the beacon factor graph is shown, this is an overly complicated representation since the position p is assumed to be known. This makes it so that the β values are known and a factor graph for each antenna can be used, as shown in Figure 3.3. In this per antenna factor graph, the phase β can be calculated using

$$\beta_m = -2\pi \frac{\sin(\theta) d_{rx}}{\lambda}(m-1) \text{ for } m = 1, 2, \ldots, N, \tag{3.4}$$

where the AoA θ is dependent on the position of the transmitter as well as the position of the antenna array.

With this, it ends up being a simple calculation of the messages since there are no loops involved. The only issue is that while β and ϕ both are phases and the phase of y can be measured the additive noise n is not. However if one assumes a high SNR scenario, in the same way as for the MAP estimator in Section 2.3.2, a simple Gaussian approximation can be done. The function node f_{y_m} will be given as

$$f_{y_m}(y_m, \phi_m, \beta_m, n_m) = \delta(\phi_m + \beta_m + \angle n_m - \angle y_m).$$

The calculations of the means and variance for the messages then become

$$\eta_{f_{n_m}-n_m}(n_m) = [0, \sigma_n^2]^T$$
$$\eta_{f_{\phi_m}-\phi_m}(\phi_m) = [\mu_{\phi_m}, \sigma_\phi^2]^T$$
$$\eta_{y_m-f_{y_m}}(y_m) = [\angle y_m, 0]^T$$

$$\eta_{n_m-f_{y_m}}(n_m) = [0, \sigma_n^2]^T$$

$$\eta_{f_{y_m}-\phi_m}(\phi_m) = [\angle y_m - \beta_m, \frac{\sigma_n^2}{2}]^T.$$

The above messages are all that is needed, and lastly the marginal of the random phase ϕ_m can be calculated. In the beacon case, the message $\eta_{f_{\phi_m}-\phi_m}(\phi_m)$ can be discarded since there is initially no prior information about it, which is the same as setting the variance in the message to infinity. Then the mean and variance end up being

$$\mu_{\phi_m} = \angle y_m - \beta_m \tag{3.5}$$
$$\sigma_{\phi_m}^2 = \frac{\sigma_n^2}{2}. \tag{3.6}$$

This is shown to give a good approximation of the true distribution as long as the signal power is much larger than the noise power.

3.3 Factor graph for position estimate

The factor graph in Figure 3.4 displays the connection between all the parameters involved in the estimation of the position. In this figure, it is assumed that there is a given prior for the position, which is necessary to avoid spatial folding problems. The random phase at each antenna is also assumed to have a given distribution, which is the one found from the beacon factor graph. Both of these factor graphs could technically be put into one, but for simplicity, they are kept separate.

Below all the function nodes and priors are described. The prior for the random phase at each antenna array k and each antenna m is assumed to be the marginal found in the estimation for the random phase. This is again assumed to be a continuous normal distribution, which is correct for a high SNR beacon scenario. The function in node f_ϕ is then given by the prior for the random phase as

$$f_\phi(\phi_{km}) = P(\phi_{km}) = g(\phi_{km}) = N(\mu_{\phi_{km}}, \sigma_{\phi_{km}}^2).$$

The noise is still assumed to be complex Gaussian, and the noise power can be different at each of the antenna arrays k, and the function node f_n is then given by

$$f_n(n_{km}) = P_n(n_{km}) = N(0, \sigma_{kn}^2).$$

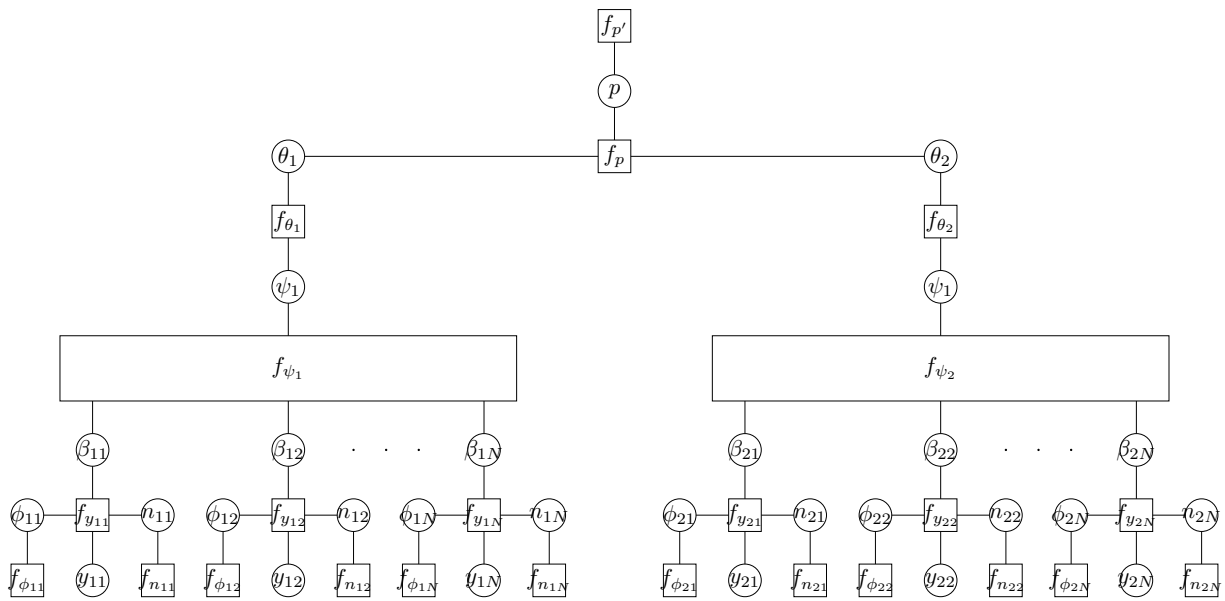

Figure 3.4: Factor graph, Total system

There is assumed to be given some prior of the position, this can be as a multivariate normal distribution as

$$f_{p'}(\boldsymbol{p}) = N(\mu_{\boldsymbol{p}}, \Sigma_p).$$

In an ideal scenario the two coordinates would not be dependant and the covariance matrix would be a diagonal matrix.

The rest of the function nodes are defined by the dependencies between the variables which are done through the use of delta functions and the function nodes f_y, f_θ and f_p are given as

$$f_{y_{km}}(y_{km}, \phi_{km}, \beta_{km}, n_{km}) = \delta(\beta_{km} + \phi_{km} + \angle n_{km} - \angle y_{km})$$

$$f_{\theta_k}(\psi_k, \theta_k) = \delta(\psi_k + 2\pi \frac{\sin(\theta_k) d_{rx}}{\lambda})$$

$$f_p(\theta_1, \theta_2, \boldsymbol{p}) = \delta\left(\theta_1 - \left(\frac{\pi}{2} - \arctan\left(\frac{p_y - y_1}{p_x - x_1}\right) - \theta_{1r}\right)\right)\delta\left(\theta_2 - \left(-\frac{\pi}{2} - \arctan\left(\frac{p_y - y_2}{p_x - x_2}\right) - \theta_{2r}\right)\right).$$

The last function node that is missing is the node that does processing on an input vector f_{ψ_k}, this function takes the information from all of the antennas and then produce a single estimate for the phase rotation ψ_k. This function cannot be described by a simple function but is a type of iterative estimation as all of the β depend on the phase rotation ψ, which causes a lot of dependencies and therefore loops. A description of this function is done in the following section for the calculations of the messages going upwards.

What follows is the calculations of all the messages first the ones going upwards and then the downwards messages, this is assuming the position node is the top as in Figure 3.4. They are also separated into the steps for each "wave" of the messages.

3.3.1 Message-Passing

Upward messages

Step 1 The two first messages will always be Gaussian distributions since they are just the prior distributions that are given and these messages can, therefore, be just the mean and variance of each of them.

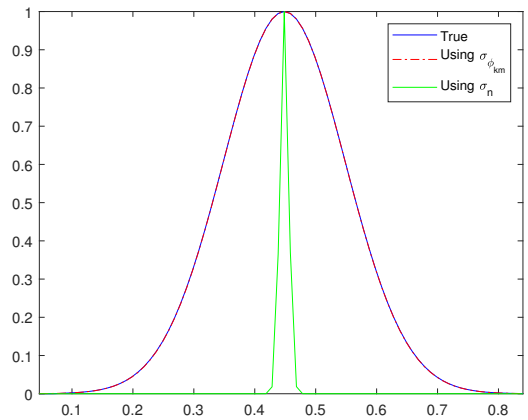

Figure 3.5: Distribution of the message in step 3, the true value and gaussian approximations

As mentioned before to differentiate the gaussian messages from the distribution messages the notation $\eta_{node1-node2}$ for the messages is used. The messages in this step are then given by

$$\eta_{f_n-n_{km}}(n_{km}) = [0, \sigma_n]$$
$$\eta_{f_\phi-\phi_{km}}(\phi_{km}) = [\mu_{\phi_{km}}, \sigma_{\phi_{km}}]$$
$$\eta_{y_{km}-f_{y_{km}}}(y_{km}) = y_{km}.$$

Step 2 As described in Section 3.1 the messages simply propagate through the variable nodes, when they only have two connections. The messages then simply become

$$\eta_{n_{km}-f_{y_{km}}}(n_{km}) = [0, \sigma_n]$$
$$\eta_{\phi_{km}-f_{y_{km}}}(\phi_{km}) = [\mu_{\phi_{km}}, \sigma_{\phi_{km}}].$$

Step 3 When calculating the message that is going upwards from the function node f_y there are some considerations that must be done. Since the distribution of the noise n is in the complex domain and the random phase ϕ is not, one cannot directly combine these and get the message. In Figure 3.5 the true distribution of the outgoing message is shown together with the distribution when assuming the phase variance dominates and when the noise variance dominates. This shows that if the phase variance is much larger then that of the noise it is reasonable to discard it and in the opposite case if the noise variance is much larger then the phase variance, which is not shown here, the results show that one can discard the phase variance. It is, therefore, reasonable to assume that either the noise or the phase error dominates and can be used to calculate the message.

Using this the true messages can be calculated as

$$\eta_{f_{y_{km}}-\beta_{km}}(\beta_{km}) = [\mu_{\beta_{km}}, \sigma_{\beta_{km}}].$$

Where $\mu_{\beta_{km}} = wrapToPi(\angle(y_{km}) - \mu_{\phi_{km}})$ and $\sigma_{\beta_{km}} = max(\frac{\sigma_n}{\sqrt{2}}, \sigma_{\phi_{km}})$. The wrapping to π is done to keep all the results within the same limits which is what one could find from the phase of a received signal. The assumption with taking the maximum holds as long as the two values are not equal or really close.

Step 4 Same as before the variable nodes simply propagate the same messages to the next function node and the message is given by

$$\eta_{\beta_{km}-f_{\psi_m}}(\beta_{km}) = [\mu_{\beta_{km}}, \sigma_{\beta_{km}}].$$

Step 5 In this step, all of the messages coming from each of the antennas are combined to get one estimate of the phase rotation ψ_k. This is as mentioned before a complex process and there are a lot of dependencies. The true value of each β_{km} is given as

$$\beta_{km} = \psi_k(m-1).$$

Where ψ_k is the true phase rotation and where $m = 1, 2, 3 \ldots N$ is the antenna number.

From this one can see that it would be desirable to find the phase difference between two antennas as far apart as possible since we then have a variance of the estimate of ψ_k which scales with $\frac{1}{m^2}$. The phase difference between the first and last antenna as well as the estimated phase rotation ψ_k and its variance is then given by

$$\begin{aligned} \beta_{kN} - \beta_{k1} &= (N-1)\psi_k \\ \psi_k &= \frac{\beta_{kN} - \beta_{k1}}{N-1} \\ Var(\psi_k) &= \frac{1}{(N-1)^2}(Var(\beta_{kN}) + Var(\beta_{k1})). \end{aligned} \tag{3.7}$$

This would then give a really good result, it is however not possible to do this directly since the phase at each antenna wraps down to a value between $-\pi$ and π. An iterative method is, therefore, necessary to be able to estimate the unwrapped phase and from that the phase rotation. This method can be described using the factor graph in Figure 3.6, which shows how the estimate from Equation 3.7 can be found. The message passing in this graph is really simple. What is essentially done is first estimating the phase rotation ψ_1' with the difference in phase between adjacent antennas. Then the phase difference between antennas with one antenna in between is found $\psi_{m(m+2)}$, this will give several possible phases, because of phase wrapping, the previous estimate for the phase rotation ψ_1' is then used to decide which one of these is most likely to be correct. All of these phases are then used to estimate a new ψ_2'. This is then done iteratively increasing the number of antennas in between each time and estimating a new ψ_l' each time.

The method then becomes doing the calculations until there is an estimate for phase rotation ψ_{1N} from the unwrapped phase difference between antenna 1 and antenna N. This could be used as the estimate for the phase rotation, but during these calculations, there are other independent estimates for the phase rotation. For all the estimates to be independent one can only use information from each antenna once, this then gives the independent estimates $[\psi_{1N}, \psi_{2(N-1)}, \psi_{3(N-2)}, \ldots, \psi_{\frac{N}{2}(\frac{N}{2}+1)}]$ all with a standard deviation given by the distance between the antennas. Using these estimates, one can take a weighted average and get the final estimate for the phase rotation ψ. The mean and standard deviation for the message that is sent from this function node further up the factor graph is then given as

$$\mu_{\psi_k} = \frac{\sum_{m=1}^{N/2} \frac{\psi_{m(N-m+1)}}{\sigma^2_{\psi_{m(N-m+1)}}}}{\sum_{m=1}^{N/2} \frac{1}{\sigma_{\psi^2_{m(N-m+1)}}}} \tag{3.8}$$

$$\sigma_{\psi_k} = \sqrt{\frac{1}{\sum_{m=1}^{N/2} \frac{1}{\sigma_{\psi^2_{m(N-m+1)}}}}}, \tag{3.9}$$

which gives the message

$$\eta_{f_{\psi_k} - \psi_k}(\psi_k) = [\mu_{\psi_k}, \sigma_{\psi_k}].$$

Step 6 Again the message is just propagated in this step and the message is then given as

$$\eta_{\psi_k - f_{\theta_k}}(\psi_k) = [\mu_{\psi_k}, \sigma_{\psi_k}].$$

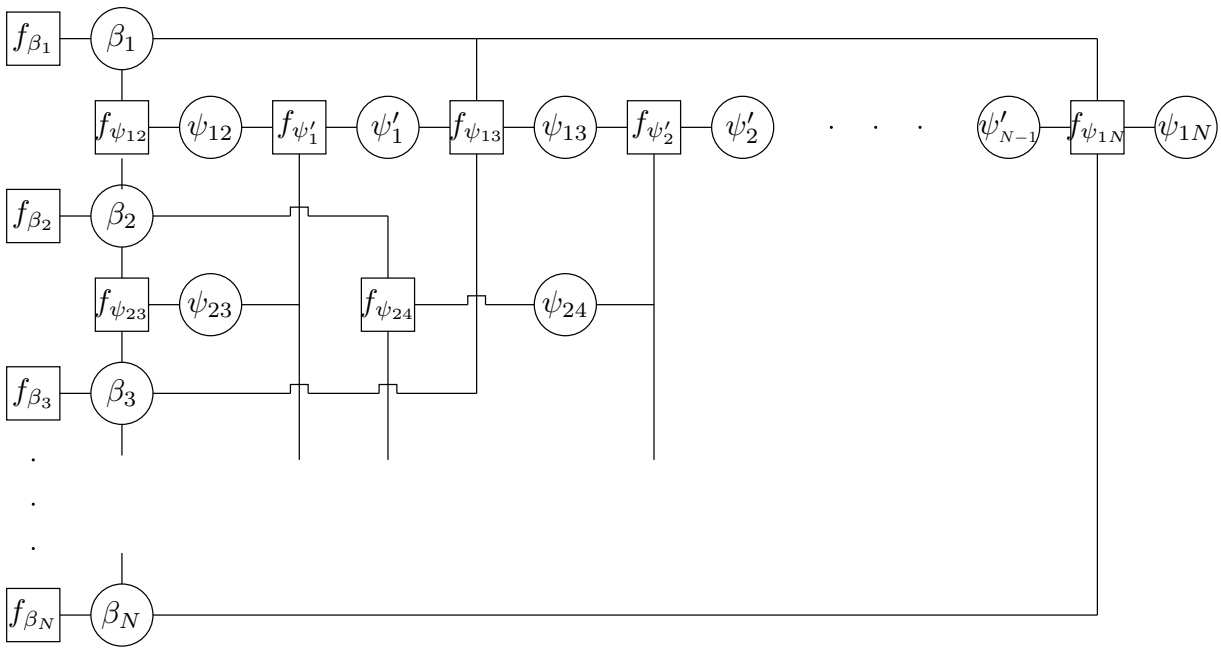

Figure 3.6: Factor graph, part of the estimation of the random phase ψ_k

Step 7 The next function node f_θ is again a simple mapping but through a non-linear function. As described previously in the AoA section these functions can be linearized using a Taylor expansion. The function in the node is given by

$$\theta_k = \text{asin}\left(-\frac{\psi_k \lambda}{2\pi d_{rx}}\right).$$

In this step one also have to take into account the wrapping caused by the antenna spacing. This will introduce the possibility of several angles giving the phase shift observed. The number of possibilities is given by $\frac{2d_{rx}}{\lambda}$. The way to find all the possible angles is to find the maximum phase shift one could get when the AoA is between $-\pi/2$ and $\pi/2$, which would be $2\pi\frac{d_{rx}}{\lambda}$. To find all the different angles one then simply create a vector with the found phase and add or subtract 2π until the maximum phase shift is reached both with a negative and positive phase.

The Taylor expansion is then given by

$$\hat{\theta}_k = \text{asin}\left(-\frac{\boldsymbol{\mu_{\psi_k}}\lambda}{2\pi d_{rx}}\right) + (\psi_k - \boldsymbol{\mu_{\psi_k}})\frac{\frac{\lambda}{2\pi d_{rx}}}{\sqrt{1-(\frac{\lambda}{2\pi d_{rx}})^2 \boldsymbol{\mu_{\psi_k}}^2}}.$$

For the message this gives the simple calculations and the mean, standard deviation and message is given as

$$\boldsymbol{\mu_{\theta_k}} = \text{asin}\left(-\frac{\boldsymbol{\mu_{\psi_k}}\lambda}{2\pi d_{rx}}\right)$$

$$\boldsymbol{\sigma_{\theta_k}} = \sigma_{\psi_k}\frac{\frac{\lambda}{2\pi d_{rx}}}{\sqrt{1-(\frac{\lambda}{2\pi d_{rx}})^2 \boldsymbol{\mu^2_{\psi_k}}}}$$

$$\eta_{f_{\theta_k}-\theta_k}(\theta_k) = [\boldsymbol{\mu_{\theta_k}}, \boldsymbol{\sigma_{\theta_k}}].$$

With the message then including several possible AoA as well as their corresponding variance.

Step 8 The message is just propagated in this step and the message is then given as

$$\eta_{\theta_k - f_{\boldsymbol{p}}}(\theta_k) = [\boldsymbol{\mu_{\theta_k}}, \boldsymbol{\sigma_{\theta_k}}].$$

Step 9 In the last step upwards in the factor graph, there is another non-linear mapping to a position, which has to done for all the possible AoA. As described in Section 2.3.3 and using the equations that were calculated there, it gives simple calculations. One does, however, need to map from AoA at the antenna arrays to the α and β used in the Taylor expansion, this gives the simple mapping given as

$$\alpha = \frac{\pi}{2} - \theta_1 - \theta_{1r}$$
$$\beta = \frac{\pi}{2} + \theta_2 + \theta_{2r}.$$

Their means are also simply expressed as

$$\boldsymbol{\mu_\alpha} = \frac{\pi}{2} - \boldsymbol{\mu_{\theta_1}} - \theta_{1r}$$
$$\boldsymbol{\mu_\beta} = \frac{\pi}{2} + \boldsymbol{\mu_{\theta_2}} + \theta_{2r}.$$

This then gives the calculations for the variances, covariance and means given from Equation 2.27, 2.28, 2.29, 2.23 and 2.24 as

$$\boldsymbol{\sigma}^2_{p_x} = (\frac{\partial p_x}{\partial \alpha}(\boldsymbol{\mu_\alpha}, \boldsymbol{\mu_\beta}))^2 \boldsymbol{\sigma^2_{\theta_1}} + (\frac{\partial p_x}{\partial \beta}(\boldsymbol{\mu_\alpha}, \boldsymbol{\mu_\beta}))^2 \boldsymbol{\sigma^2_{\theta_2}}$$
$$\boldsymbol{\sigma}^2_{p_y} = (\frac{\partial p_y}{\partial \alpha}(\boldsymbol{\mu_\alpha}, \boldsymbol{\mu_\beta}))^2 \boldsymbol{\sigma^2_{\theta_1}} + (\frac{\partial p_y}{\partial \beta}(\boldsymbol{\mu_\alpha}, \boldsymbol{\mu_\beta}))^2 \boldsymbol{\sigma^2_{\theta_2}}$$
$$\boldsymbol{Cov}(p_x, p_y) = (\frac{\partial p_x}{\partial \alpha}(\boldsymbol{\mu_\alpha}, \boldsymbol{\mu_\beta}))(\frac{\partial p_y}{\partial \alpha}(\boldsymbol{\mu_\alpha}, \boldsymbol{\mu_\beta}))\boldsymbol{\sigma^2_{\theta_1}} + (\frac{\partial p_x}{\partial \beta}(\boldsymbol{\mu_\alpha}, \boldsymbol{\mu_\beta}))(\frac{\partial p_y}{\partial \beta}(\boldsymbol{\mu_\alpha}, \boldsymbol{\mu_\beta}))\boldsymbol{\sigma^2_{\theta_2}}$$

$$\boldsymbol{\mu_{p_x}} = p_x(\boldsymbol{\mu_\alpha}, \boldsymbol{\mu_\beta})$$
$$\boldsymbol{\mu_{p_y}} = p_y(\boldsymbol{\mu_\alpha}, \boldsymbol{\mu_\beta}).$$

Downward messages

Step 1 In the first step, the prior for the position is simply propagated, and since we are assuming a Gaussian distribution the actual message will be its means and the covariance matrix

$$\eta_{f_{p'} - \boldsymbol{p}}(\boldsymbol{p}) = [\boldsymbol{\mu_p}, \Sigma_{p'}]^T.$$

Step 2 The variable node just propagate the message as

$$\eta_{\boldsymbol{p} - f_p}(\boldsymbol{p}) = [\boldsymbol{\mu_p}, \Sigma_{p'}]^T.$$

Step 3 In this step what is essentially done is a reverse of the angle to position Taylor expansion given before. One does, however, need the distribution of both the position and the other AoA to find one of the AoAs. Using Equation 2.23 and 2.24 there can be found two equations for each of the means as

$$\mu_\alpha = \arctan\left(\frac{\tan(\mu_\beta)(\frac{x_2}{\mu_{p_x}} - 1)}{1 - \frac{x_1}{\mu_{p_x}}}\right)$$
$$\mu_\alpha = \arctan\left(\frac{\tan(\mu_\beta)}{\frac{x_2 - x_1}{\mu_{p_y}}\tan(\mu_\beta) - 1}\right)$$

$$\mu_\beta = \arctan\left(\frac{\tan(\mu_\alpha)(\frac{x_1}{\mu_{p_x}} - 1)}{1 - \frac{x_2}{\mu_{p_x}}}\right)$$

$$\mu_\beta = \arctan\left(\frac{\tan(\mu_\alpha)}{\frac{x_2 - x_1}{\mu_{p_y}}\tan(\mu_\alpha) - 1}\right).$$

As the equations show there are two equations for each mean because one could use both the x- and the y-position to calculate it. These should give the same result, but can also be averaged.

Using the equations for the standard deviations and covariance matrix in Equation 2.27, 2.28 and 2.29 in step nine downwards one can calculate three equations for each of the variances as

$$\sigma_\alpha^2 = \frac{\sigma_{p_x}^2 - \sigma_\beta^2(\frac{\partial p_x}{\partial \beta})^2}{(\frac{\partial p_x}{\partial \alpha})^2}$$

$$\sigma_\alpha^2 = \frac{\sigma_{p_y}^2 - \sigma_\beta^2(\frac{\partial p_y}{\partial \beta})^2}{(\frac{\partial p_y}{\partial \alpha})^2}$$

$$\sigma_\alpha^2 = \frac{Cov(p_x, p_y) - \sigma_\beta^2(\frac{\partial p_x}{\partial \beta})(\frac{\partial p_y}{\partial \beta})}{(\frac{\partial p_x}{\partial \alpha})(\frac{\partial p_y}{\partial \alpha})}$$

$$\sigma_\beta^2 = \frac{\sigma_{p_x}^2 - \sigma_\alpha^2(\frac{\partial p_x}{\partial \alpha})^2}{(\frac{\partial p_x}{\partial \beta})^2}$$

$$\sigma_\beta^2 = \frac{\sigma_{p_y}^2 - \sigma_\alpha^2(\frac{\partial p_y}{\partial \alpha})^2}{(\frac{\partial p_y}{\partial \beta})^2}$$

$$\sigma_\beta^2 = \frac{Cov(p_x, p_y) - \sigma_\alpha^2(\frac{\partial p_x}{\partial \alpha})(\frac{\partial p_y}{\partial \alpha})}{(\frac{\partial p_x}{\partial \beta})(\frac{\partial p_y}{\partial \beta})}.$$

Using all this together with the converting from α and β to θ_1 and θ_2. We have the message going downwards, where the mean and variance is an average of the different values calculated, given as

$$\eta_{f_{\boldsymbol{p}} - \theta_k}(\theta_k) = [\boldsymbol{\mu_{\theta_k}}, \boldsymbol{\sigma_{\theta_k}}].$$

Step 4 The variable node just propagate the message as

$$\eta_{\theta_k - f_{\theta_k}}(\theta_k) = [\boldsymbol{\mu_{\theta_k}}, \boldsymbol{\sigma_{\theta_k}}].$$

Step 5 In the same way, as in the upwards propagation in this node, there is a need for a Taylor expansion. Which is given by

$$\hat{\psi}_{km} = 2\pi\frac{\sin(\mu_{\theta_k})d_{rx}}{\lambda} + (\theta_k - \mu_{\theta_k})2\pi\frac{\cos(\mu_{\theta_k})d_{rx}}{\lambda}.$$

Since there could be several possible angles because of spatial folding, all of these need to be taken into account. They do however produce the same phase rotation ψ and they can simply be averaged out. This gives the equations for the mean and standard deviation given by

$$\mu_{\psi_{km}} = mean(2\pi\frac{\sin(\boldsymbol{\mu_{\theta_k}})d_{rx}}{\lambda})$$

$$\sigma_{\psi_{km}} = mean(\boldsymbol{\sigma_{\theta_k}} 2\pi \frac{\cos(\boldsymbol{\mu_{\theta_k}}) d_{rx}}{\lambda}).$$

And the message is then given as

$$\eta_{f_{\theta_k} - \psi_k}(\psi_k) = [\mu_{\psi_k}, \sigma_{\psi_k}].$$

Step 6 The variable node just propagate the message as

$$\eta_{\psi_k - f_{\psi_k}}(\psi_k) = [\mu_{\psi_k}, \sigma_{\psi_k}].$$

Step 7 For this step, all the incoming messages have to be used to calculate each of the messages going out. This means the messages calculated in upwards step 4 has to be used. Then using the fact that the phase rotates with the phase rotation ψ_k between each antenna one can use a weighted mean and get an estimate for the phase β at each antenna. The mean and standard deviation is then given as

$$\mu_{\beta_{km}} = \frac{\sum_{n \neq m} \frac{\beta_{kn} - (n-m)\mu_{\psi_k}}{\sigma_{\beta^2_{kn}} + (n-k)^2 \sigma^2_{\psi_k}}}{\sum_{n \neq m} \frac{1}{\sigma_{\beta^2_{kn}} + (n-k)^2 \sigma^2_{\psi_k}}}$$

$$\sigma_{\beta_{km}} = \sqrt{\frac{1}{\sum_{n \neq m} \frac{1}{\sigma_{\beta^2_{kn}} + (n-k)^2 \sigma^2_{\psi_k}}}},$$

where the notation $n \neq m$ means to sum over all possible n except $n = m$. The message is then simply given as

$$\eta_{f_{\psi_k} - \beta_{km}}(\beta_{km}) = [\mu_{\beta_{km}}, \sigma_{\beta_{km}}]$$

Step 8 The variable node just propagate the message as

$$\eta_{\beta_{km} - f_{y_k m}}(\beta_{km}) = [\mu_{\beta_{km}}, \sigma_{\beta_{km}}].$$

Step 9 In the same way, as in the upwards pass, the calculations in node $f_{y_k m}$ are essential given by if the variance of the incoming message is larger or smaller then the message coming from the noise when the SNR is assumed high. Which gives the mean, standard deviation and message as

$$\mu_{\phi_{km}} = wrapToPi(\angle(y_{km} - \mu_{\beta_{km}}))$$
$$\sigma_{\phi_{km}} = max(\sigma_{\frac{\sigma_n}{\sqrt{2}}, \beta_{km}})$$

$$\eta_{f_{y_k m} - \phi_{km}}(\phi_{km}) = [\mu_{\phi_{km}}, \sigma_{\phi_{km}}].$$

3.3.2 Algorithm

As mentioned in the factor graph theory the message passing algorithm becomes iterative when there are loops in the factor graph. In Figure 3.4 there are no loops, but this is because the part that has loops has been placed inside the calculations in function node f_{ψ_k}. As shown in Figure 3.6 these loops are solved by iterating from one antenna to the others to unwrap the phase and in the end, get several independent estimates of the phase. Since the loops only are internally within this node, there is no need to iterate over the whole factor graph.

Depending on how the system is used there are two different scenarios to consider. The first one is a case when the only information we want is a better estimate for the position, in which case one only needs to

calculate the messages going upwards. In the second scenario, we want to get a better estimate of the position as well as a better estimate for the random phases. In this case, one needs to first calculate all the messages going upwards and then calculate the messages going downwards.

There are therefore two different algorithms one can do, but the first one is really just stopping at an earlier point in the second one, so only the second one will be described. In Algorithm 1 the algorithm is shown, this includes the random phase estimation through the beacon. The data that the algorithm needs as input is also described, which is the geometry of the setup, the position of the beacon and a prior for the position of the transmitter (found through for example correlation).

Algorithm 1 Algorithm

Input: Geometry, Beacon position, Prior transmitter position

1: Calculate the messages in the beacon factor graph
2: Calculate posteriori distribution for the random phases
3: Calculate the upwards messages at both antenna arrays step 1-9
4: Calculate the posteriori distribution for the position
5: Calculate the downwards messages at both antenna arrays step 1-9
6: Calculate the posteriori distribution for the random phases

Chapter 4

Numerical results

4.1 System setups used in simulation

As described previously the estimation algorithm is based on the factor graph in Figure 3.3 and 3.4. These two figures define the whole system and together with the messages give the algorithm. The beacon part of the factor graph is a really simple part of the algorithm, which could be done at each of the antenna arrays separately since it does not depend on the signal received at the other antenna array. The second part of the algorithm which estimates the position of a transmitter is however more complex. As described in Section 3.3 one part of the factor graph includes loops, which requires an iterative estimation and scheduling of the calculation of messages, which is described in step 5 of upwards messages in the same section.

There are a lot of different system configurations that can be used to test the system, by changing, for example, the tilt of the antenna arrays, the position of the antenna arrays or the position of the beacon in relation to the antenna arrays. In this section, the system configuration that will be tested and done simulations on are shown.

Figure 4.1a shows a simple illustration of the first possible system setup, including the beacon and the transmitter. Here the position of the beacon is known and the position of the transmitter TX is not known. In this system setup, both of the antenna arrays are tilted at a 45° angle towards the middle and they are placed in the positions (-1000,0) and (1000,0) (in meters) for antenna array 1 and 2 respectively. The tilt was chosen to be 45° because the CRLB shows that the limit for the angle estimate is best when the AoA is normal to the antenna array. With 45° it is then expected that the best estimate would be in position (0,1000), with both AoAs being 0°.

The second configuration that will be considered is a setup similar to the previous one except that the antennas are not tilted towards each other. This setup is used to verify that the tilted scenario would give a better estimate for positions in the area around the best position (0,1000). In Figure 4.1b the setup of the system is shown. In this system setup, the antenna arrays are also placed in the positions (-1000,0) and (1000,0) (in meters) for antenna array 1 and 2 respectively.

4.2 Expected system behavior

It is possible to do some prediction about how the algorithm will behave and what kind of system setup that will be desirable to use and what kind of simulations that should be done to test the true behavior. In Section 2.2.3 the CRLB lower bound for the angle using a single antenna array was found. Using this lower bound together with the mapping to position, one can then find a lower bound for the position estimate.

Figure 4.2 shows the area of the positions that will be simulated in relation to the antenna arrays, the position of the beacon is also shown. To reduce the number of simulations required only one half of the area will be considered, but since the system is symmetric the results will be mirrored around x equals zero.

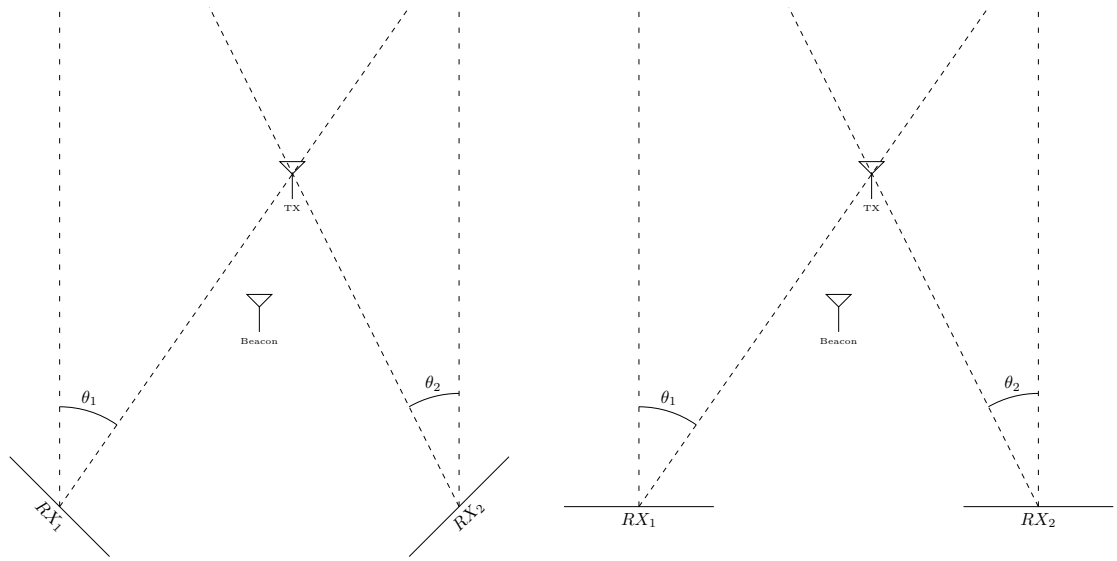

(a) Tilted antenna arrays **(b)** Flat antenna arrays

Figure 4.1: System setups

Each intersection of lines in the figure represents a position used in the simulation. In the scenario with flat antenna arrays, the arrays will be in the exact same position only not tilted, similar to the difference between Figure 4.1a and 4.1b.

In Figure 4.3 the lower bound for the root mean square (RMS) error for mentioned positions is shown, using 900 MHz carrier frequency, antenna spacing of 4λ, 64 antennas, transmitter SNR of 15 dB, antenna array 1 in position (-1000,0), antenna array 2 in position (1000,0) and with tilted antenna arrays. As expected this shows that the best estimates are in the middle when both of the angles are the lowest and that when the angle increases the limit goes higher. Figure 4.4 also shows the lower bound, only here the SNR is no longer constant and varies assuming a free-space loss model, this shows the same results as the previous figure only here the positions further away gets a higher limit and the closer positions a lower limit as expected.

The same limit can be found using the flat antenna arrays, in Figure 4.5 and 4.6 the limit is shown with constant SNR and using a free-space loss model respectively. These figures show that this system configuration shows slightly different behavior. In this configuration, the best position is still the middle, but now the worst position is closer to the antenna arrays this can be explained by that the angle in this configuration is much larger at those positions than in the tilted configuration. And as expected when the free-space loss model is introduced one gets worse at the further positions and better at the closer positions.

It would also be interesting to predict how the system would behave dependent on both the SNR of the signal from the transmitter and the SNR of the signal from the beacon, which from now is noted as transmitter SNR and beacon SNR respectively. When one looks at the calculations for the factor graph in Section 3.3, the function in upwards step 3 shows that it sends a message with the maximum of the standard deviation for the random phase and the standard deviation for the noise divided by two. This indicates that as long as the standard deviation for the noise divided by two is the largest getting a better estimate of the random phase will not give a better estimate. This can be expressed as an inequality using these two standard deviations, which is given as

$$\sigma_\phi^2 \leq \frac{\sigma_n^2}{2}.$$

Which when substituting with the beacon and transmitter SNRs on a linear scale gives

$$\frac{1}{2SNR_{beacon}} \leq \frac{1}{2SNR_{transmitter}}$$

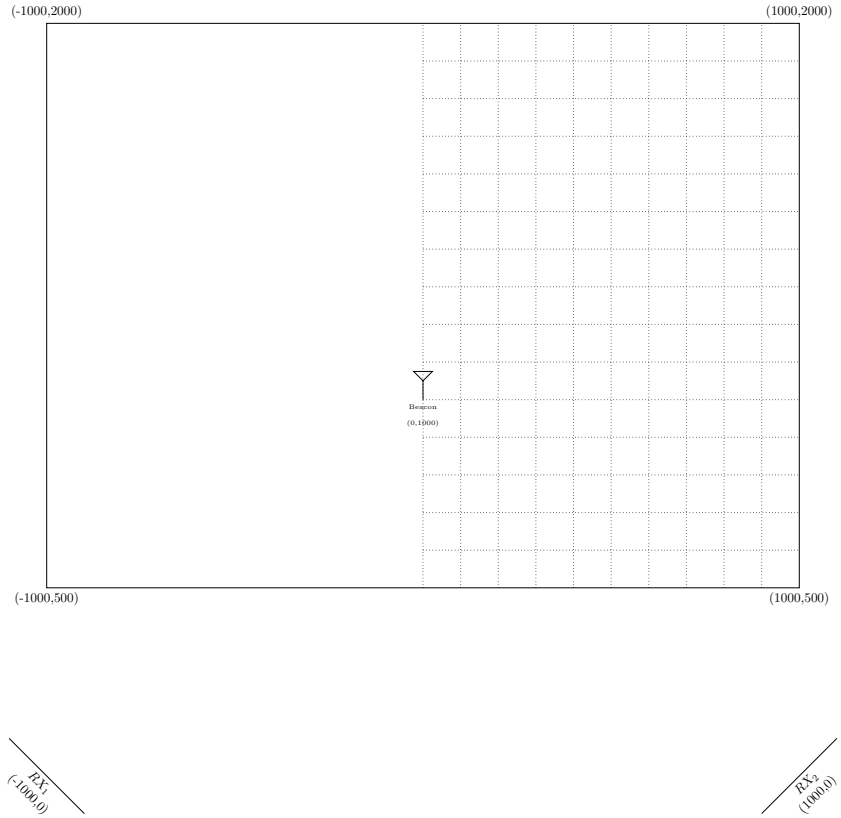

Figure 4.2: Simulated positions in relation to the antenna arrays and beacon

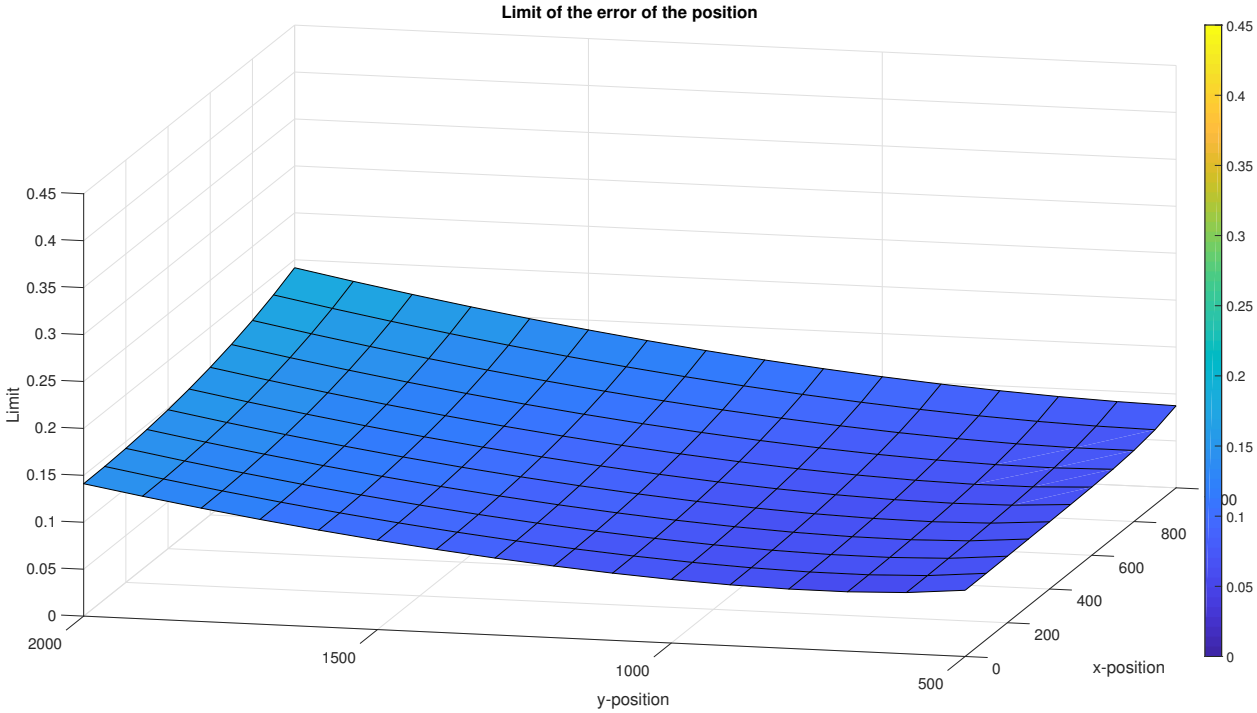

Figure 4.3: The Cramer-Rao lower bound for each position with a received transmitter SNR of 15 dB

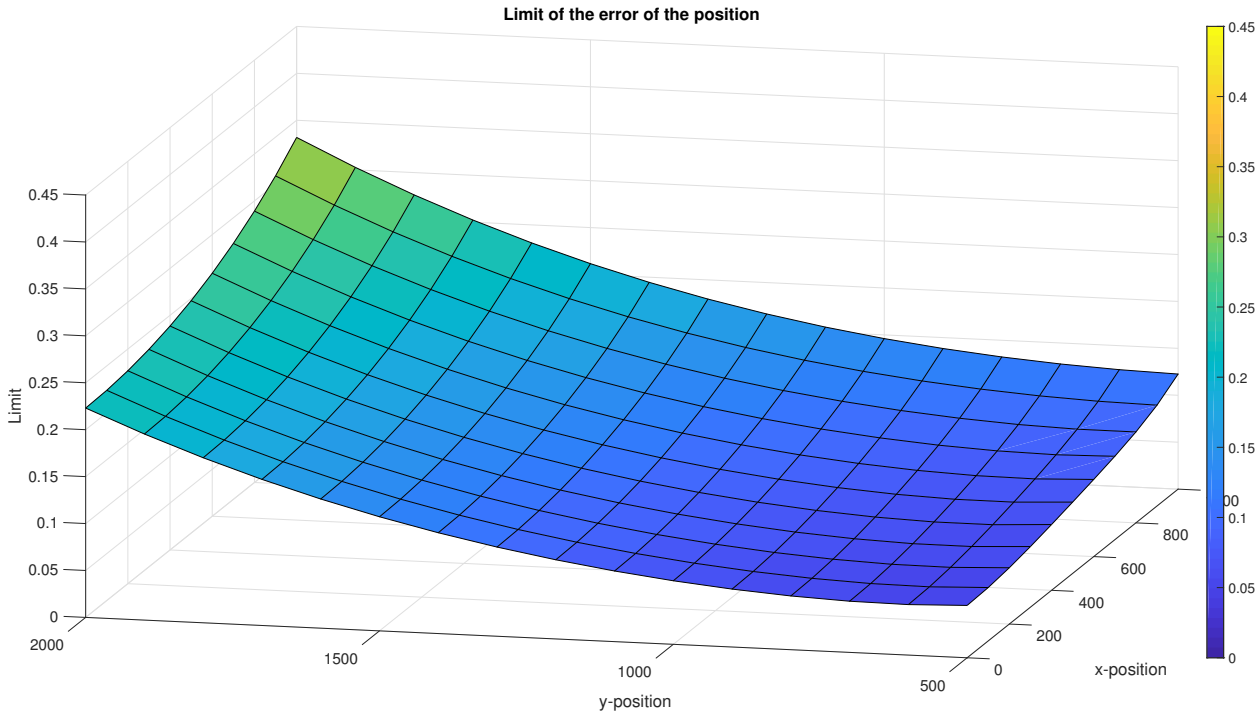

Figure 4.4: The Cramer-Rao lower bound for each position with a received transmitter SNR varying with free-space loss with a SNR of 15 at position (0,1000)

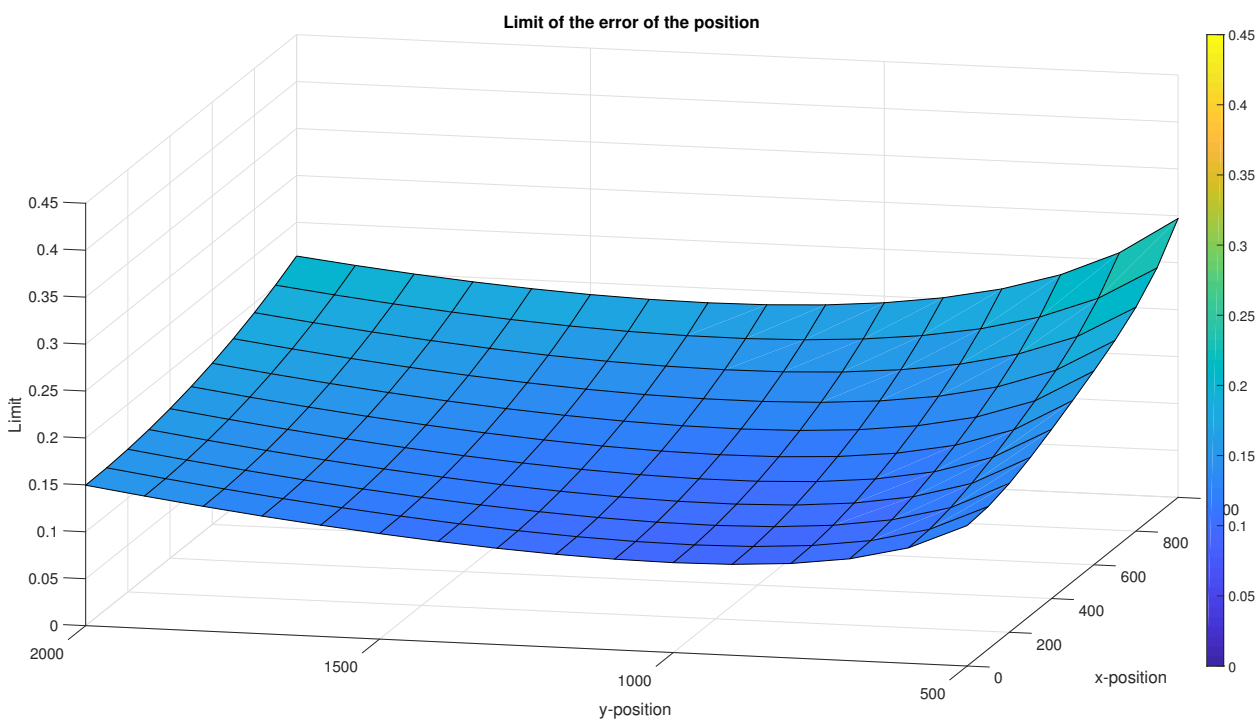

Figure 4.5: The Cramer-Rao lower bound for each position with a received transmitter SNR of 15 dB

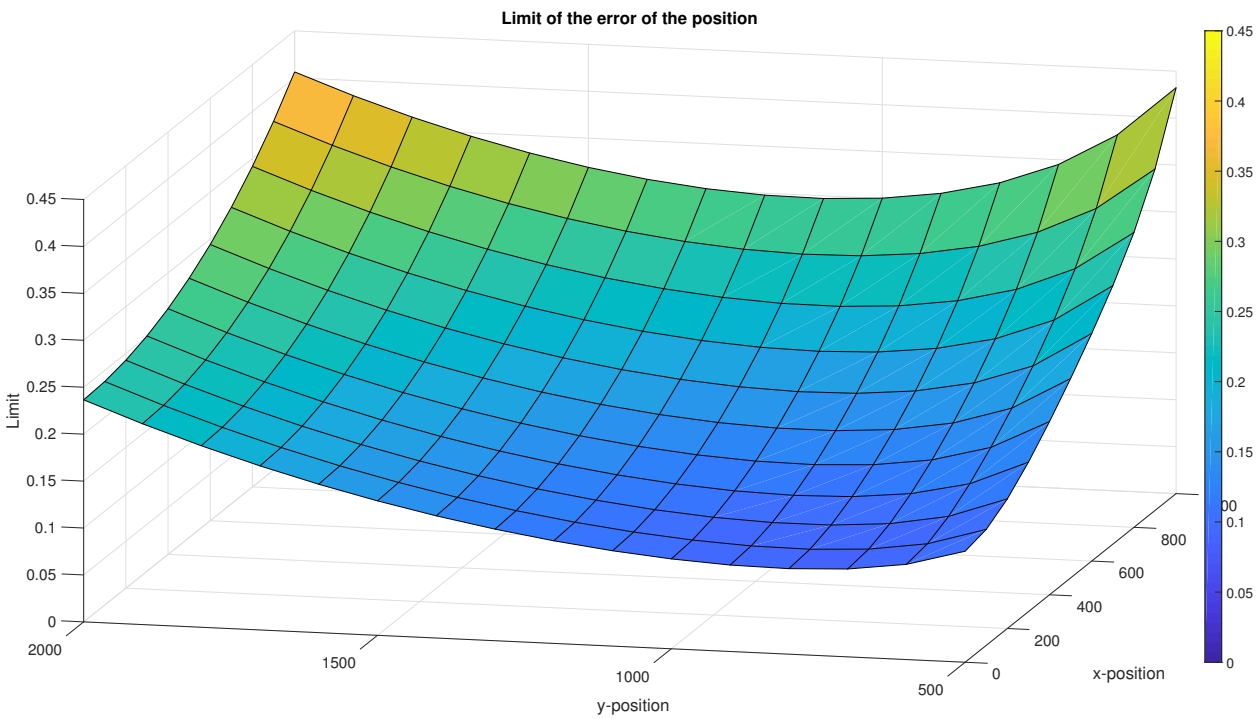

Figure 4.6: The Cramer-Rao lower bound for each position with a received transmitter SNR varying with free-space loss with a SNR of 15 at position (0,1000)

$$SNR_{beacon} \geq SNR_{transmitter}. \tag{4.1}$$

Equation 4.1 shows that as long as the beacon SNR is larger then the transmitter SNR one would always propagate the standard deviation from the signal noise, and one would expect the system to behave similarly to a phase aligned system.

It would also be interesting to be able to predict at what point the system breaks down, with the result not just being wrong but converging to the wrong value in the iterative part. The iterative process described in upwards step 5 in Section 3.3, shows that the system uses an estimated phase difference ψ_l' to decide which unwrapped phase difference is correct. In this system, if the first estimate is bad one would choose the wrong phase wrapped version, which would propagate through the rest of the process.

Assuming the standard deviation of β at each antenna is equal it can be shown that the standard deviation of the lth estimate of ψ_l' in Figure 3.6 will be given as

$$\sigma_{\psi_l'} = \frac{1}{\sqrt{l}(N-l)}\sqrt{2}\sigma_\beta, \text{ for l<N/2} \tag{4.2}$$

$$\sigma_{\psi_l'} = \frac{1}{l\sqrt{N-l}}\sqrt{2}\sigma_\beta, \text{ for l}\geq\text{N/2}, \tag{4.3}$$

where the separation into two is done because before estimate N/2 of ψ_l' some antennas are used more than once, causing dependencies.

The equations above hold as long as the beacon SNR is high enough, which means that the standard deviation of β needs to be low enough. Figure 4.7 shows the estimated and true standard deviation of the estimate of ψ_1' for different transmitter SNRs, the two plots are of the same results with different limits. This shows that for low SNRs Equation 4.2 no longer holds. This is most likely caused by the fact that the priors for the phase β are assumed Gaussian and when the standard deviation becomes too high it causes wrapping making the distribution less gaussian.

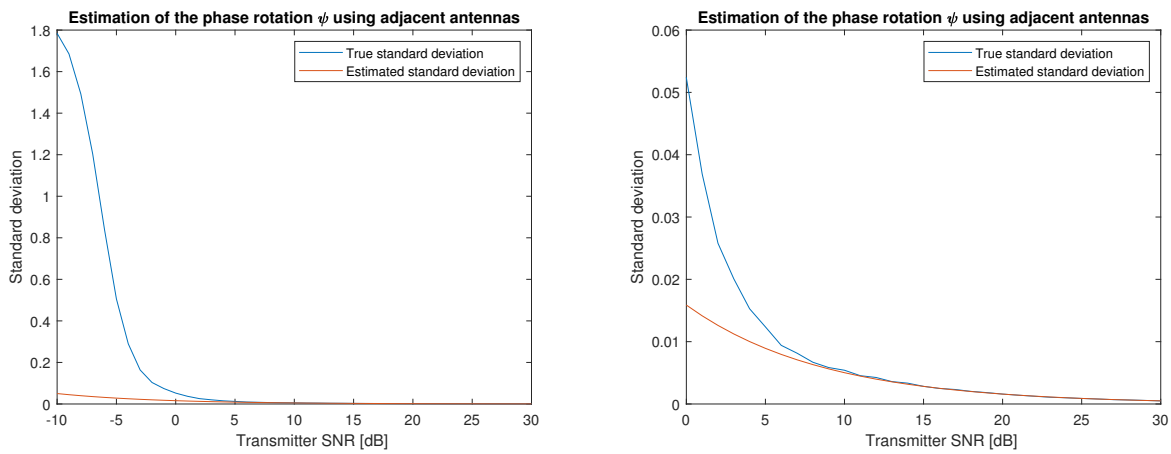

Figure 4.7: The true and estimated standard deviation of the phase rotation ψ when using phase difference between adjacent antennas and with the true phase rotation being equal 0, found using 1000 Monte-Carlo simulations.

It could be possible to get an indication of at which point this becomes a problem and if one assumes that as long as 99.9% of the Gaussian stays within 2π as the limit, one get the inequality

$$3.08\sigma_\beta \leq \pi. \tag{4.4}$$

This can then be solved for σ_β and substitute for the transmitter SNR, when assuming that the beacon SNR is much higher than the transmitter SNR, with the SNR being on a linear scale. (The same calculations can be done assuming the opposite and will give the same results with SNR_{beacon} instead of $SNR_{transmitter}$) The inequality then becomes

$$\frac{\sigma_n}{\sqrt{2}} \leq \frac{\pi}{3.08} \tag{4.5}$$

$$\frac{1}{\sqrt{2SNR_{transmitter}}} \leq \frac{\pi}{3.08} \tag{4.6}$$

$$\sqrt{2SNR_{transmitter}} \geq \frac{3.08}{\pi} \tag{4.7}$$

$$SNR_{transmitter} \geq \frac{3.08^2}{2\pi^2}. \tag{4.8}$$

When converting this to decibel one then gets the inequality

$$SNR_{transmitter} \geq -3.1823 \text{ dB}. \tag{4.9}$$

This value of -3.1823 dB is an indication for when the algorithm starts having issues, that is caused by the distribution no longer being Gaussian. As long as one is above this SNR, for both transmitter and beacon, one avoids the issue with 99.9% certainty. When comparing to the graph in Figure 4.7 -3.1823 dB seems to fit well with the start of the steeper part, but the problem seems to start at an even higher SNR, around 5 dB.

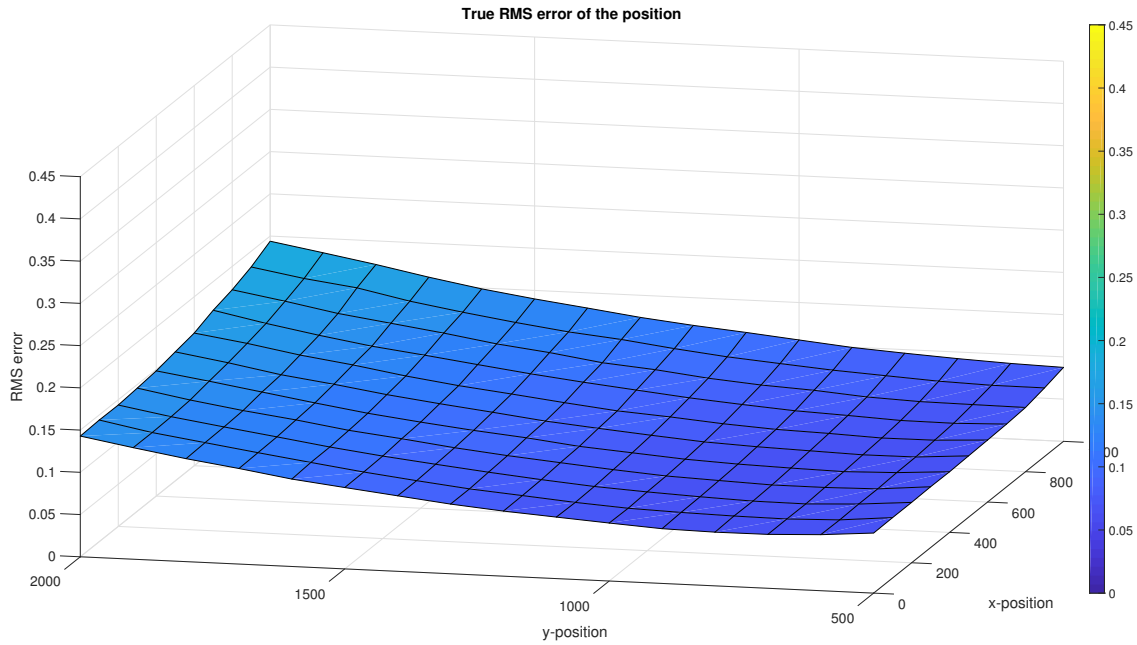

Figure 4.8: The true RMS error of the estimated position found through 10000 Monte-Carlo simulations with carrier frequency of 900 MHz, antenna spacing of 4λ, 64 antennas, transmitter SNR of 15 dB, beacon SNR of 40 dB, antenna array 1 position (-1000,0), antenna array 2 position (1000,0), antenna array 1 tilt $\pi/4$ and antenna array 2 tilt $-\pi/4$

4.3 Simulation results

To test the system several simulations were done on the systems described in the previous chapter, these simulations were done in Matlab using Monte-Carlo simulations and both the estimated position and the estimated variance of that position were compared with the true values. First all the system configurations were tested to see how the position of the transmitter changed the estimated position, then the same system was tested for different beacon SNR, then simulations were done to see if there were some requirements for the signal or beacon SNR and lastly simulations with an even larger antenna distance were done to test the effects of spatial folding.

4.3.1 Simulation for different positions

The figures in Section 4.2 show how the CRLB changes for different positions and give an indication of what positions should give better or worse estimates than others. It is therefore of interest to see if the algorithm produce similar behavior for both of the system configurations described. Same as for the lower bound the area tested is shown in Figure 4.2 in relation to the antenna arrays.

In Figure 4.8 the true variance of the estimated position measured given from the Monte-Carlo simulations. This figure shows how the precision of the estimate change for different positions. Figure 4.9 shows the estimated variance, which displays similar behavior to the true variance, but it does not have the same values. Figure 4.10 displays the percentage difference between the other two, with a negative value being when the estimated error is larger than the true error. In all these figures the values used were: carrier frequency 900 MHz, antenna spacing 4λ, antennas 64, transmitter SNR 15 dB, antenna array 1 position (-1000,0), antenna array 2 position (1000,0), antenna array 1 tilt $\pi/4$, antenna array 2 tilt $-\pi/4$, beacon SNR 40 dB, beacon position (0,1000), and 10000 Monte-Carlo simulations.

Figure 4.11, 4.12 and 4.13 show the same simulations as above only here the SNR of the received signal (which were constant) changes based on a free-space loss model with exactly the same SNR in the position (0,1000). This shows that the system displays the same overall behavior in the results, but with worse estimates in most positions as expected with lower SNR.

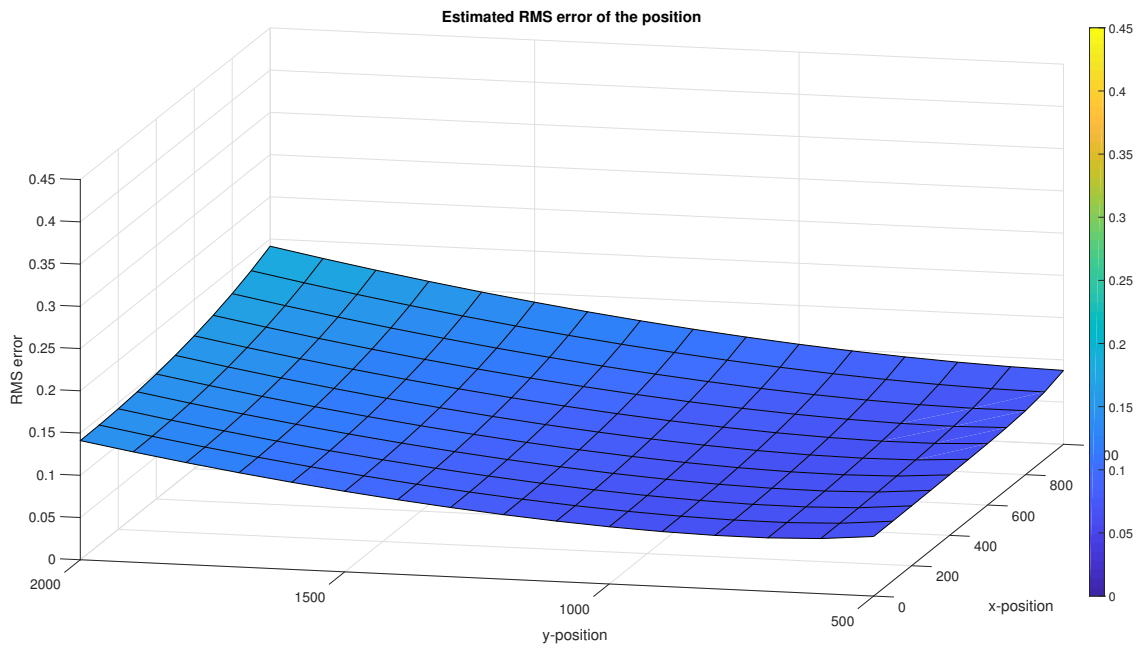

Figure 4.9: The estimated RMS error of the estimated position found through 10000 Monte-Carlo simulations with carrier frequency of 900 MHz, antenna spacing of 4λ, 64 antennas, transmitter SNR of 15 dB, beacon SNR of 40 dB, antenna array 1 position (-1000,0), antenna array 2 position (1000,0), antenna array 1 tilt $\pi/4$ and antenna array 2 tilt $-\pi/4$

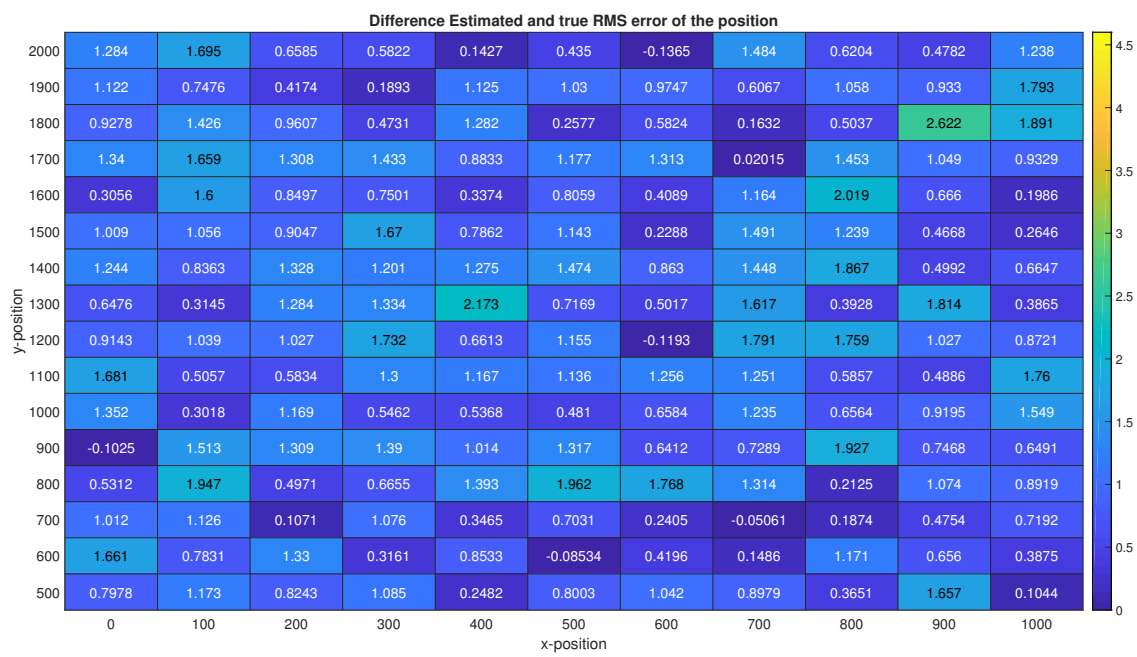

Figure 4.10: The percentage difference between the true and the estimated RMS error of the estimated position found through 1000 Monte-Carlo simulations with carrier frequency of 900 MHz, antenna spacing of 4λ, 64 antennas, transmitter SNR of 15 dB, beacon SNR of 40 dB, antenna array 1 position (-1000,0), antenna array 2 position (1000,0), antenna array 1 tilt $\pi/4$ and antenna array 2 tilt $-\pi/4$

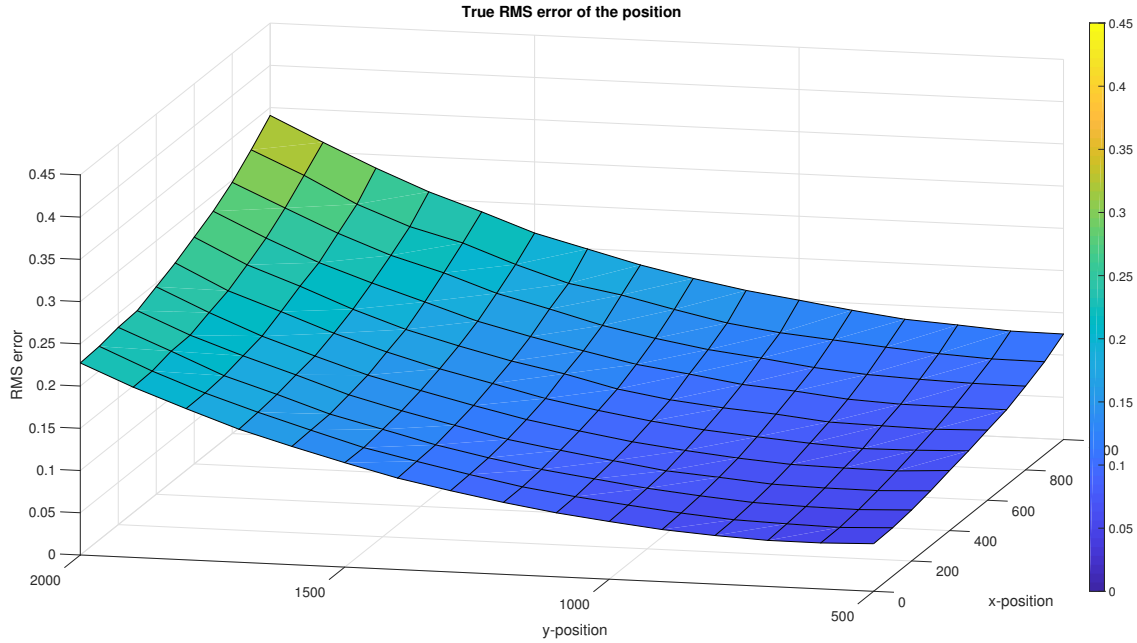

Figure 4.11: The true RMS error of the estimated position found through 1000 Monte-Carlo simulations with carrier frequency of 900 MHz, antenna spacing of 4λ, 64 antennas, transmitter SNR from a free-space loss model with SNR of 15 in position (0,1000), beacon SNR of 40 dB, antenna array 1 position (-1000,0), antenna array 2 position (1000,0), antenna array 1 tilt $\pi/4$ and antenna array 2 tilt $-\pi/4$

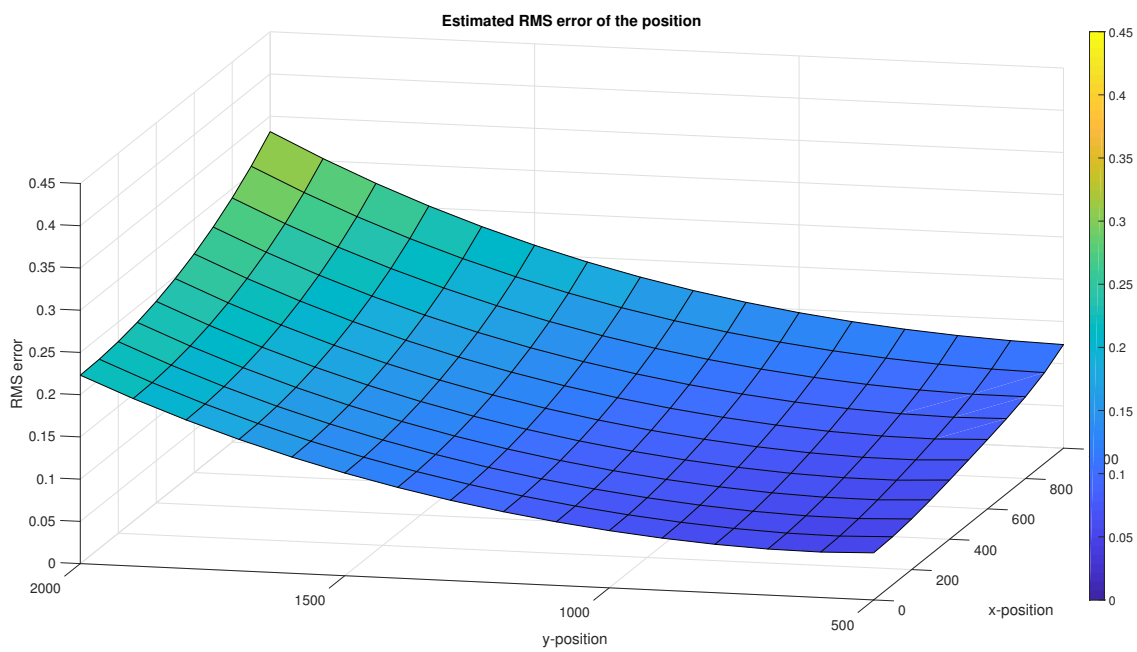

Figure 4.12: The estimated RMS error of the estimated position found through 10000 Monte-Carlo simulations with carrier frequency of 900 MHz, antenna spacing of 4λ, 64 antennas, transmitter SNR from a free-space loss model with SNR of 15 in position (0,1000), beacon SNR of 40 dB, antenna array 1 position (-1000,0), antenna array 2 position (1000,0), antenna array 1 tilt $\pi/4$ and antenna array 2 tilt $-\pi/4$

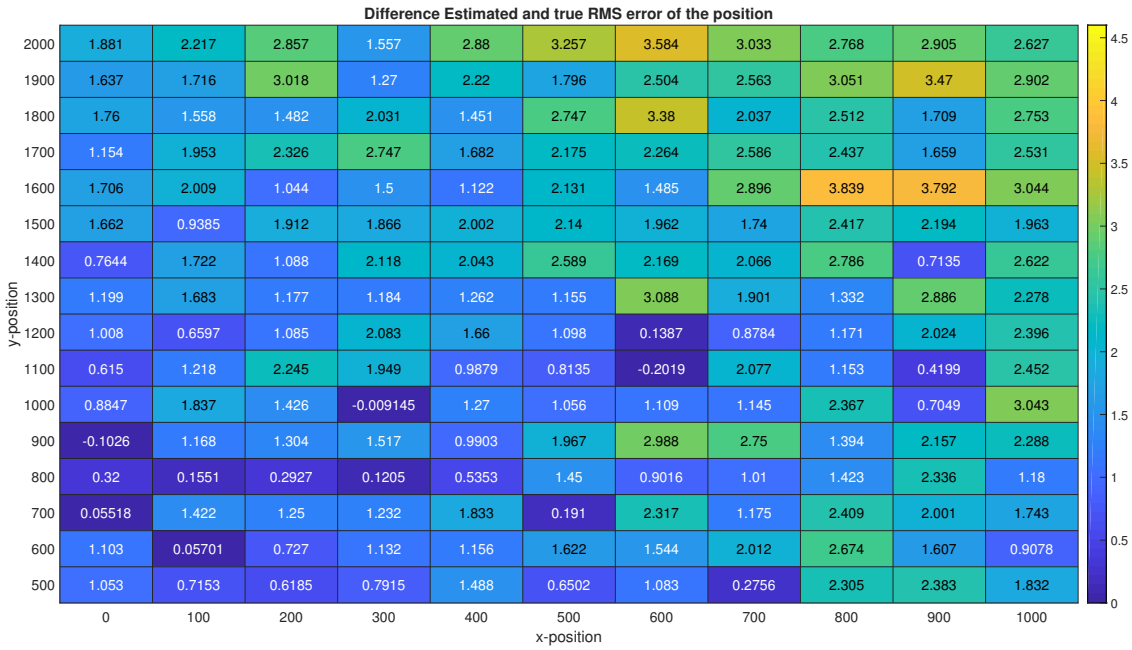

Figure 4.13: The percentage difference between the true and the estimated RMS error of the estimated position found through 10000 Monte-Carlo simulations with carrier frequency of 900 MHz, antenna spacing of 4λ, 64 antennas, transmitter SNR from a free-space loss model with SNR of 15 in position (0,1000), beacon SNR of 40 dB, antenna array 1 position (-1000,0), antenna array 2 position (1000,0), antenna array 1 tilt $\pi/4$ and antenna array 2 tilt $-\pi/4$

The system was also tested for the configuration when the antenna arrays are not tilted towards each other. Figure 4.14, 4.15, 4.16, 4.17, 4.18 and 4.19 show the same simulations as the ones done for the previous configuration in the same order and using the same values.

4.3.2 Simulation using different signal strengths

The factor graph which the algorithm is based on uses a lot of approximations as described in Section 3.3, most of these are assuming that the SNR is large, to be able to use linear approximations. It is therefore of interest to see if the system is, in fact, correct for large SNRs. It is also of interest to see if there are any points where the system approaches a phase aligned system, which would be the case if there is some point where increasing the beacon SNR no longer gives a better estimate. At the same time, it would interesting to see what kind of behavior one gets when this is no longer the case and at what SNR the system possibly breaks down.

In Figure 4.20 you can see the standard deviation for the position as a function of the SNR for the signal received from the beacon. The same Monte-Carlo simulation as for the position was done, with the same values except the position being set to (0,1000) and the beacon SNR obviously varying. In the figure, you can also see the estimated standard deviation for each SNR and the lower limit for a phase-aligned system. The two plots on the right are just the two plots on the left with different limits. The behavior seen in the two plots on the right indicates that the true SNR approach the estimated SNR and the lower limit when the beacon SNR increases. With less than 1% error in the estimated standard deviation from 30-35 dB beacon SNR. The two left plots show that at around -2 dB the true standard deviation increase drastically, indicating that the system is breaking down.

Figure 4.21 show the same simulation as in Figure 4.20, on a logarithmic scale with more lines representing different transmitter SNRs. This is done to see how the curve changes for different transmitter SNRs and if that change the point where the system behaves as a phase aligned system. For all of these graphs, the curve of the estimated value starts to flatten out and become equal to the lower limit, at the point where the variance of the random phase is equal the variance of the noise divided by two, which is what was predicted

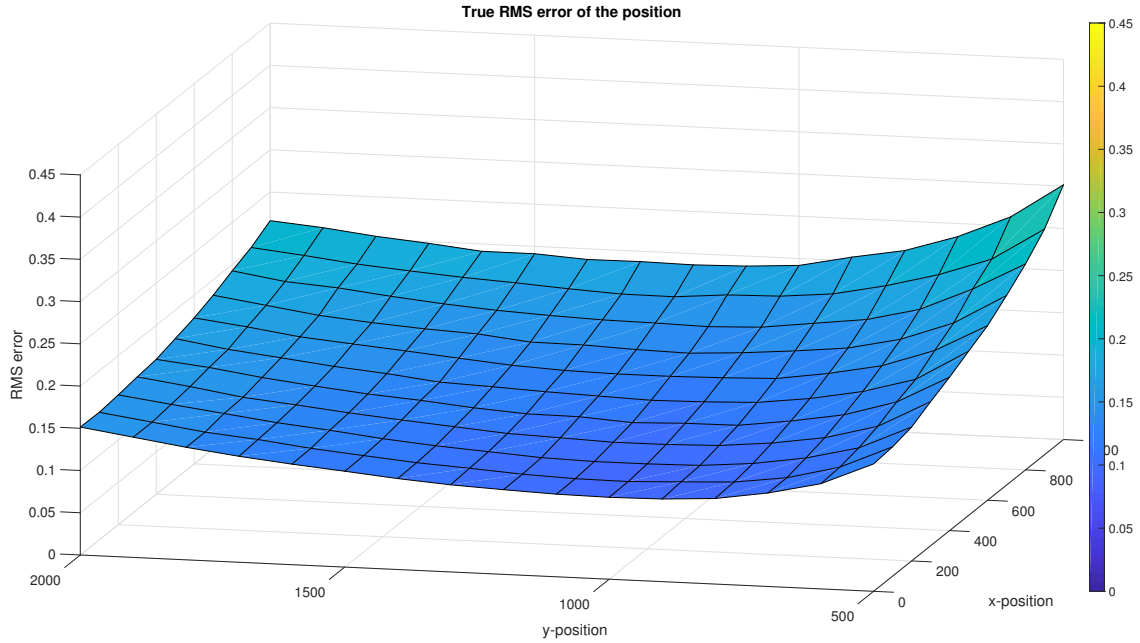

Figure 4.14: The true RMS error of the estimated position found through 10000 Monte-Carlo simulations with carrier frequency of 900 MHz, antenna spacing of 4λ, 64 antennas, transmitter SNR of 15 dB, beacon SNR of 40 dB, antenna array 1 position (-1000,0), antenna array 2 position (1000,0), antenna array 1 tilt 0 and antenna array 2 tilt 0

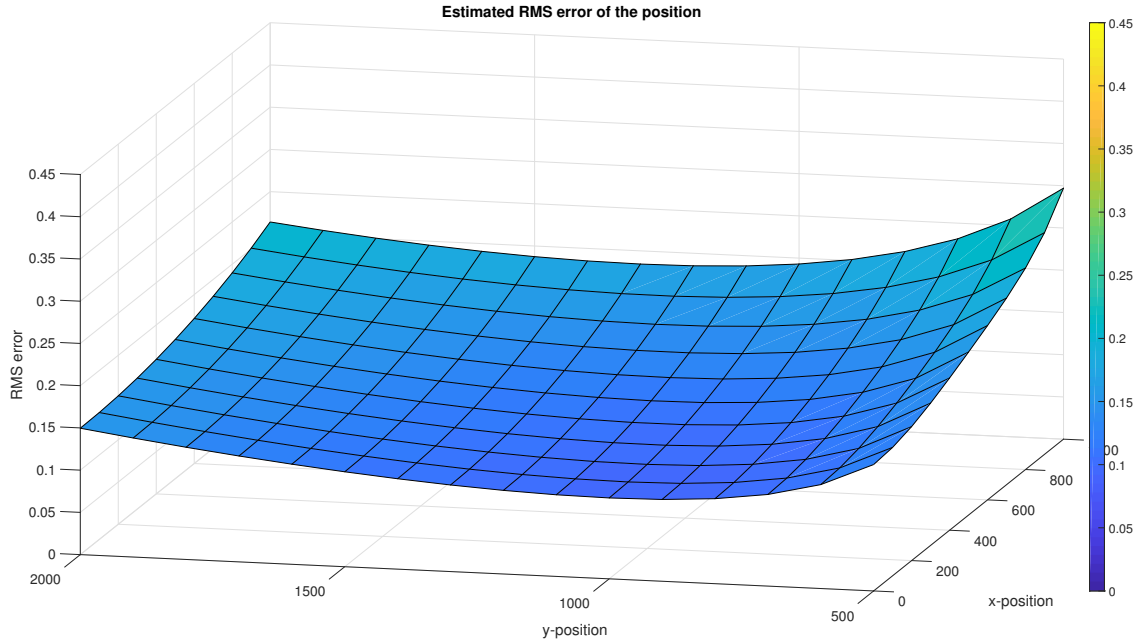

Figure 4.15: The estimated RMS error of the estimated position found through 10000 Monte-Carlo simulations with carrier frequency of 900 MHz, antenna spacing of 4λ, 64 antennas, transmitter SNR of 15 dB, beacon SNR of 40 dB, antenna array 1 position (-1000,0), antenna array 2 position (1000,0), antenna array 1 tilt 0 and antenna array 2 tilt 0

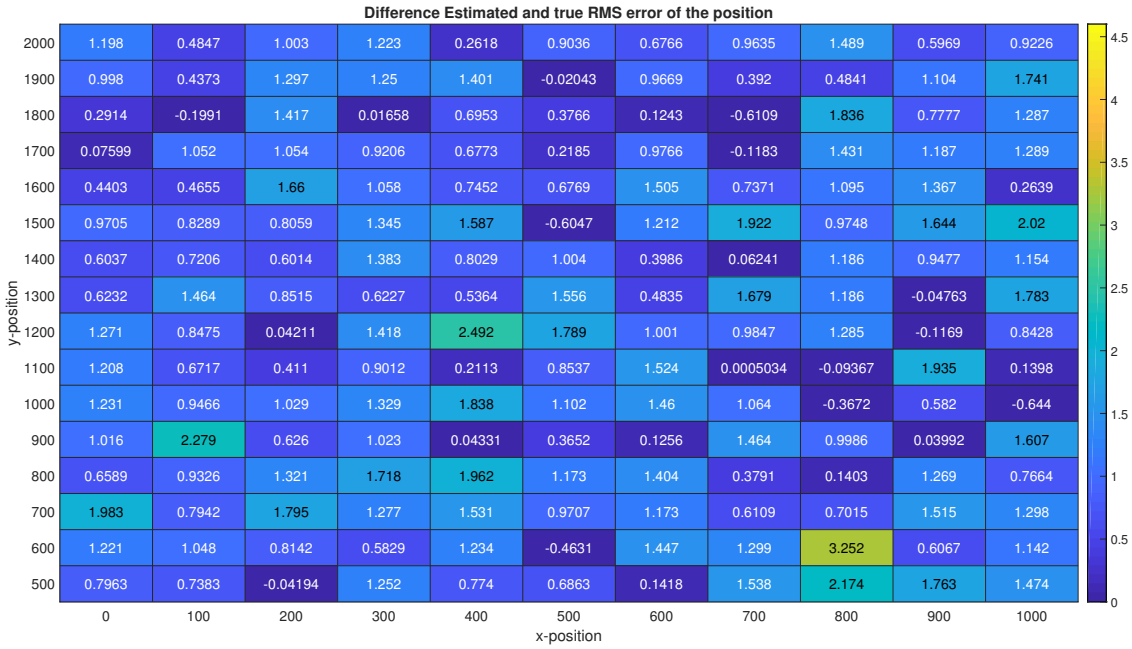

Figure 4.16: The percentage difference between the true and the estimated RMS error of the estimated position found through 10000 Monte-Carlo simulations with carrier frequency of 900 MHz, antenna spacing of 4λ, 64 antennas, transmitter SNR of 15 dB, beacon SNR of 40 dB, antenna array 1 position (-1000,0), antenna array 2 position (1000,0), antenna array 1 tilt 0 and antenna array 2 tilt 0

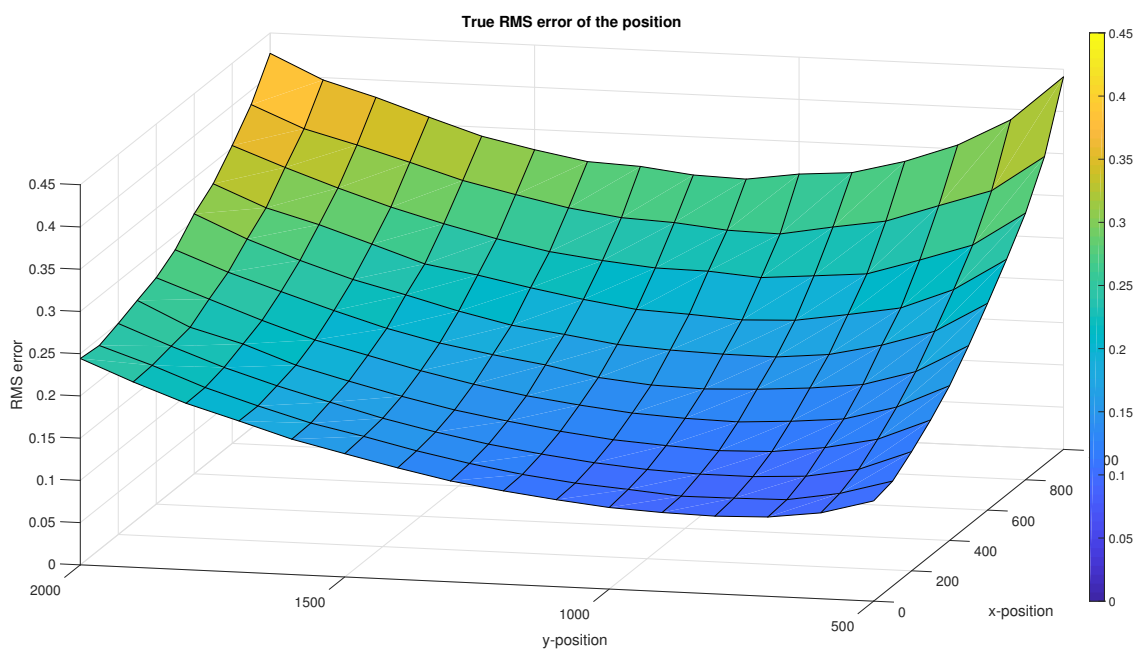

Figure 4.17: The true RMS error of the estimated position found through 10000 Monte-Carlo simulations with carrier frequency of 900 MHz, antenna spacing of 4λ, 64 antennas, transmitter SNR from a free-space loss model with SNR of 15 in position (0,1000), beacon SNR of 40 dB, antenna array 1 position (-1000,0), antenna array 2 position (1000,0), antenna array 1 tilt 0 and antenna array 2 tilt 0

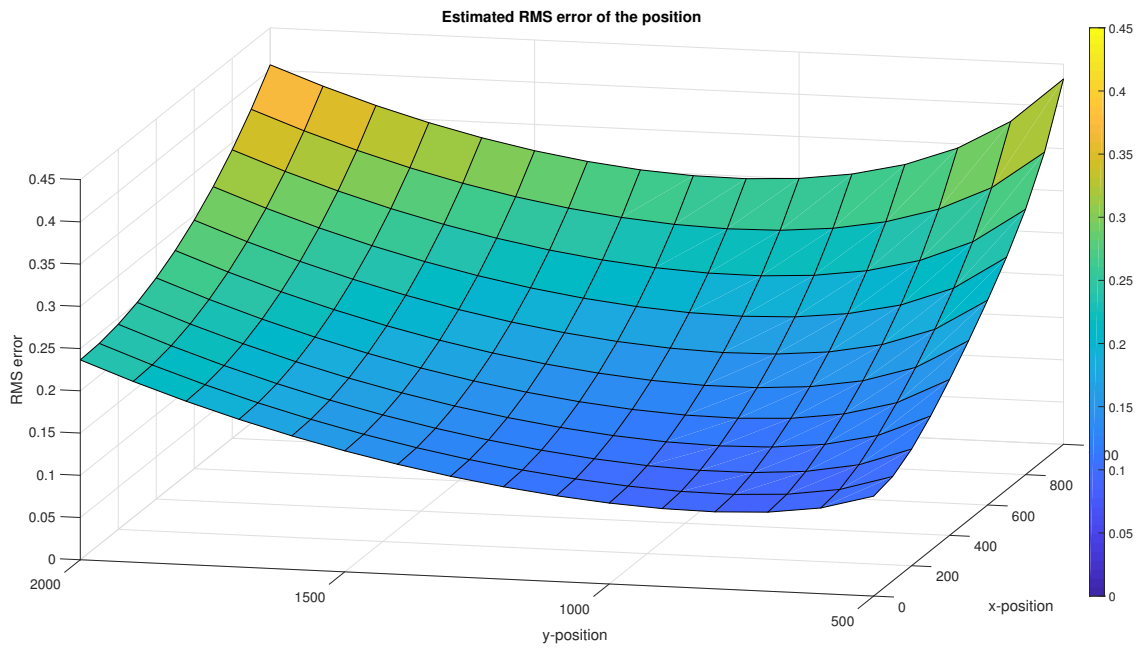

Figure 4.18: The estimated RMS error of the estimated position found through 10000 Monte-Carlo simulations with carrier frequency of 900 MHz, antenna spacing of 4λ, 64 antennas, transmitter SNR from a free-space loss model with SNR of 15 in position (0,1000), beacon SNR of 40 dB, antenna array 1 position (-1000,0), antenna array 2 position (1000,0), antenna array 1 tilt 0 and antenna array 2 tilt 0

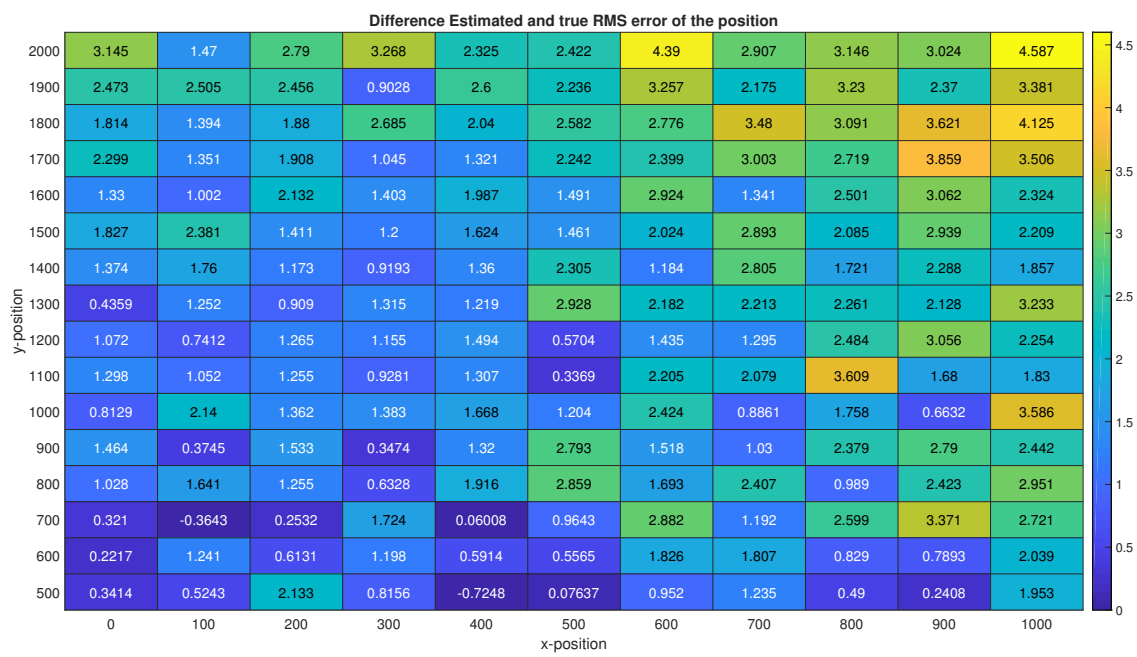

Figure 4.19: The percentage difference between the true and the estimated RMS error of the estimated position found through 10000 Monte-Carlo simulations with carrier frequency of 900 MHz, antenna spacing of 4λ, 64 antennas, transmitter SNR from a free-space loss model with SNR of 15 in position (0,1000), beacon SNR of 40 dB, antenna array 1 position (-1000,0), antenna array 2 position (1000,0), antenna array 1 tilt 0 and antenna array 2 tilt 0

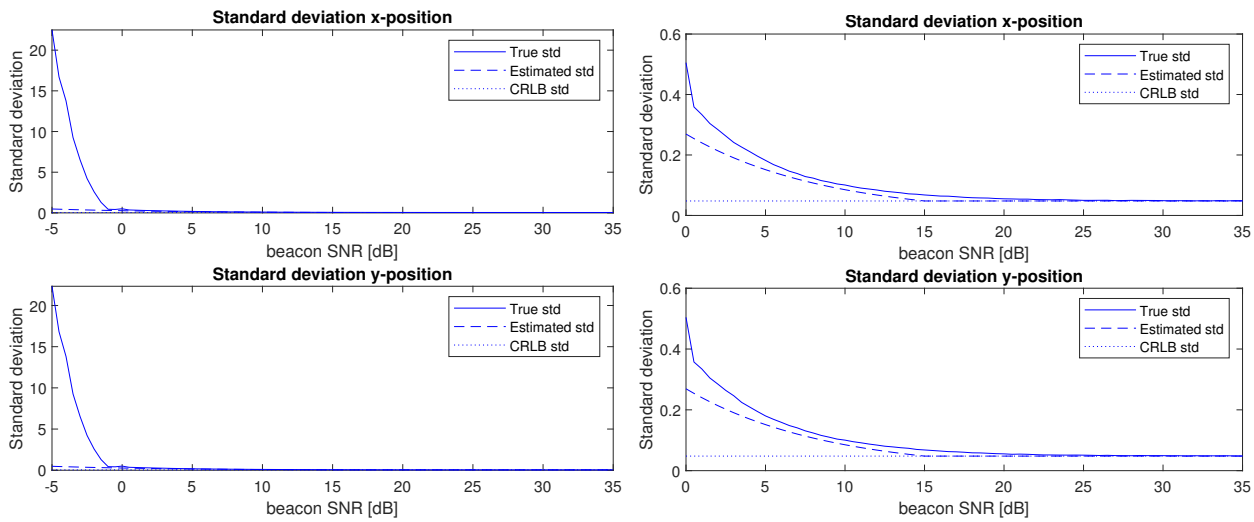

Figure 4.20: The true and estimated standard deviation of the x-and y-position found by 10000 Monte-Carlo simulations, with with carrier frequency of 900 MHz, antenna spacing of 4λ, 64 antennas, transmitter SNR of 15 dB, beacon position (0,1000), antenna array 1 position (-1000,0), antenna array 2 position (1000,0), antenna array 1 tilt $\pi/4$ and antenna array 2 tilt $-\pi/4$

in Section 4.2.

The curves of the true standard deviations, however, look like they flatten out at a slightly higher beacon SNR than the theoretically found value. Which could be because of the approximation in the upwards message passing in the first node. There it is assumed that the standard deviation of the phase and the standard deviation of the noise divided by two are not close, which they would be at the point when the SNRs are equal.

In Figure 4.22 the standard deviation of the x-position is displayed in a heatmap depending on both the beacon SNR and the transmitter SNR, the y-position gives an identical result. This shows that at around -2 dB in either of the SNRs the system breaks down and the error increases drastically. Figure 4.23 show the estimated standard deviation in the same case, which shows that it does not predict this drastic increase in error.

4.3.3 Effects of spatial folding

In Figure 4.24 and 4.25 the same simulations as previously were done only this time in some positions closer to the antenna arrays were used, as well as a larger distance between the antennas of 32λ. A logarithmic scale was also used to better see the differences in the results, the figures also have a different view angle for the same reason. This was done to see the effects of a problem that will be introduced when the prior estimate, given by correlation which is the inverse of the bandwidth times the speed of light, is too large compared to the distance between different possible positions from the spatial folding. In the estimated error it is clear that this problem is not taken into account, and as one can see from the algorithm it does not take this into account when estimating the error. This could be introduced since one knows the distance between each possible point and the uncertainty of the prior distribution, by the use of one or more Q-functions using the closest point(s).

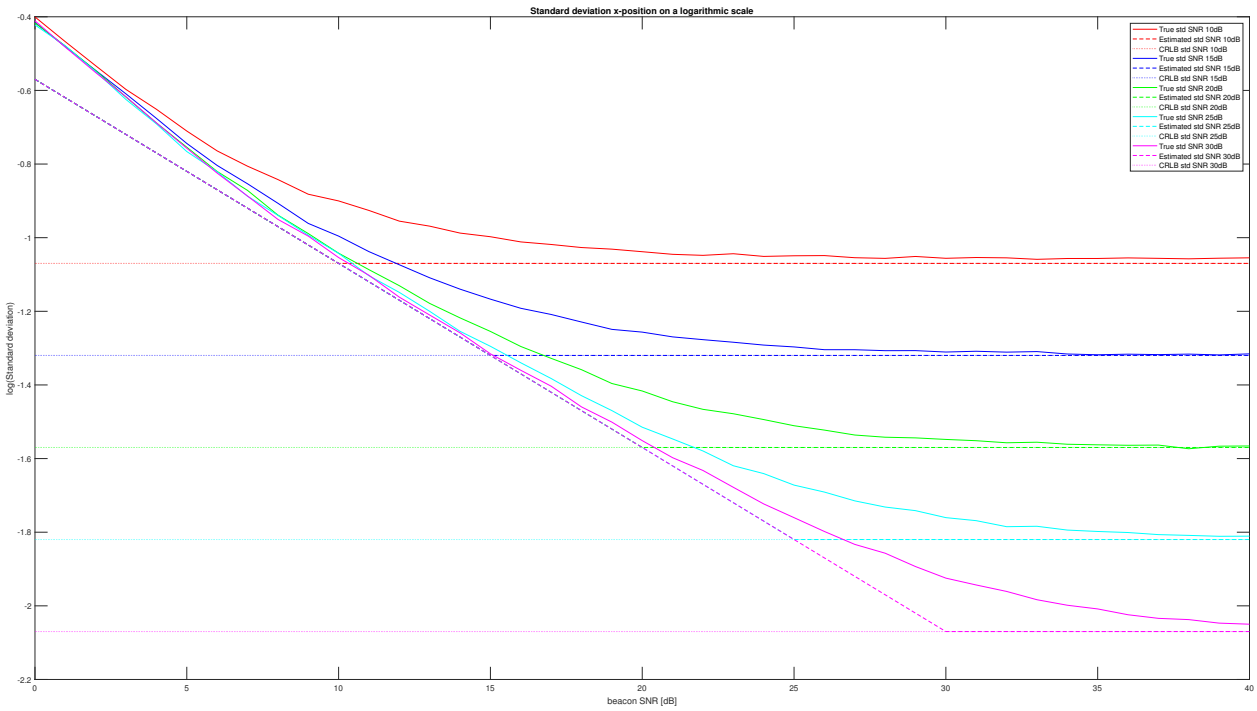

Figure 4.21: The true and estimated standard deviation on a logarithmic scale of the x-position found by 10000 Monte-Carlo simulations, with with carrier frequency of 900 MHz, antenna spacing of 4λ, 64 antennas, 10-30 dB transmitter SNR, 0-40 dB beacon SNR, beacon position (0,1000), transmitter position (0,1000), antenna array 1 position (-1000,0), antenna array 2 position (1000,0), antenna array 1 tilt $\pi/4$ and antenna array 2 tilt $-\pi/4$

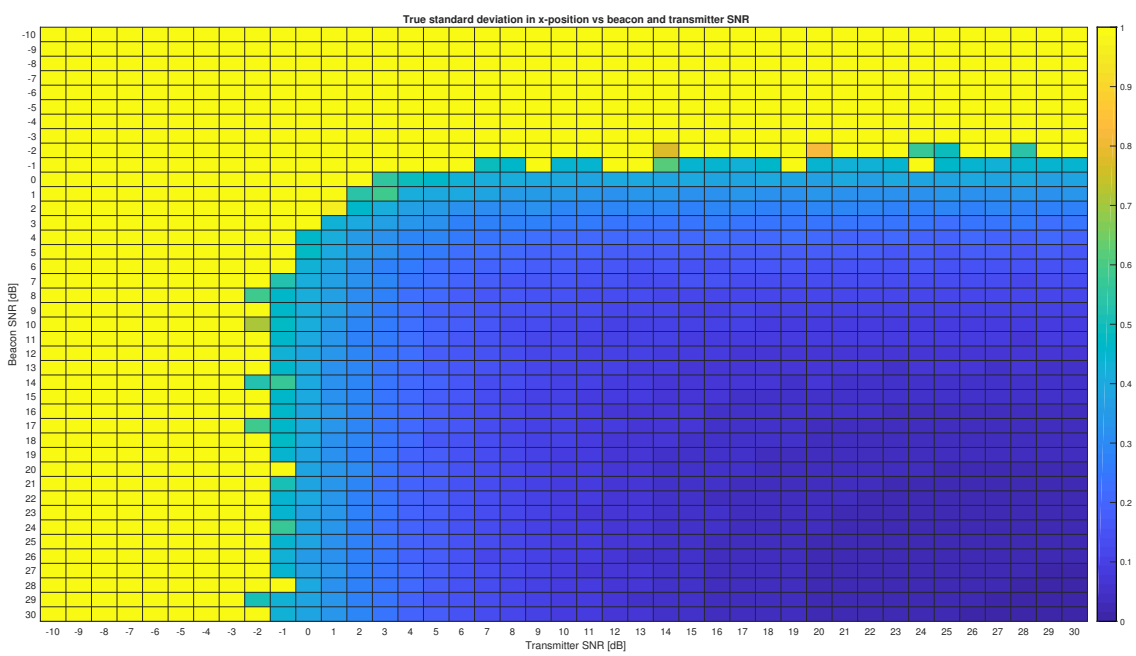

Figure 4.22: The true standard deviation of the x-position found by 1000 Monte-Carlo simulations, with with carrier frequency of 900 MHz, antenna spacing of 4λ, 64 antennas, beacon position (0,1000), transmitter position (0,1000), antenna array 1 position (-1000,0), antenna array 2 position (1000,0), antenna array 1 tilt $\pi/4$ and antenna array 2 tilt $-\pi/4$

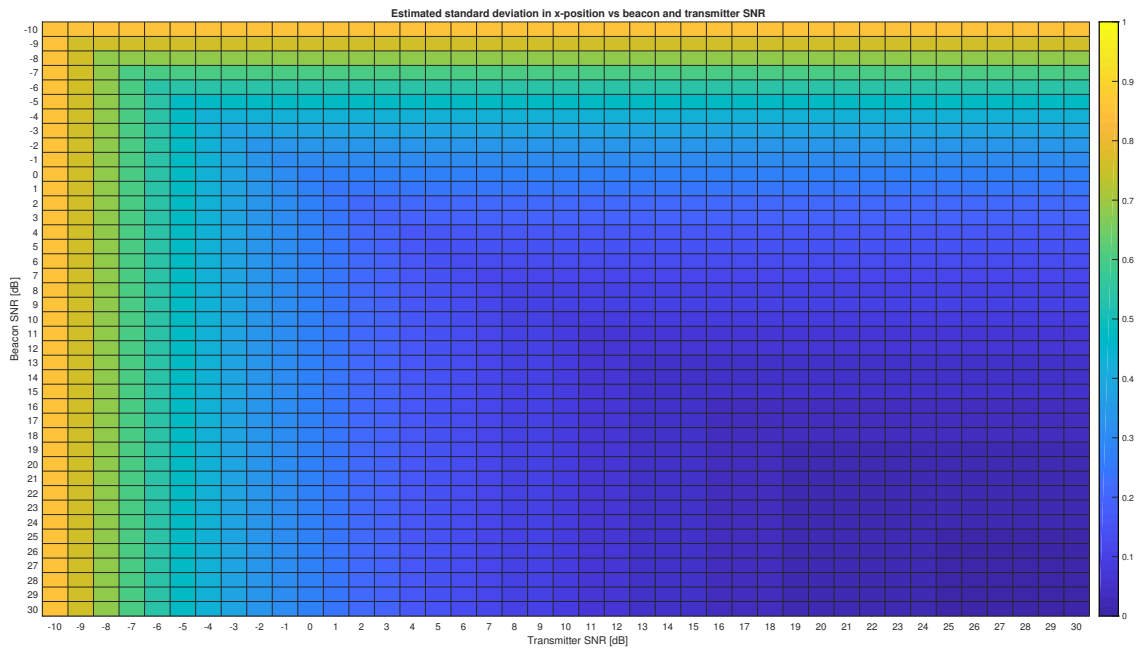

Figure 4.23: The estimated standard deviation of the x-position found by 1000 Monte-Carlo simulations, with with carrier frequency of 900 MHz, antenna spacing of 4λ, 64 antennas, beacon position (0,1000), transmitter position (0,1000), antenna array 1 position (-1000,0), antenna array 2 position (1000,0), antenna array 1 tilt $\pi/4$ and antenna array 2 tilt $-\pi/4$

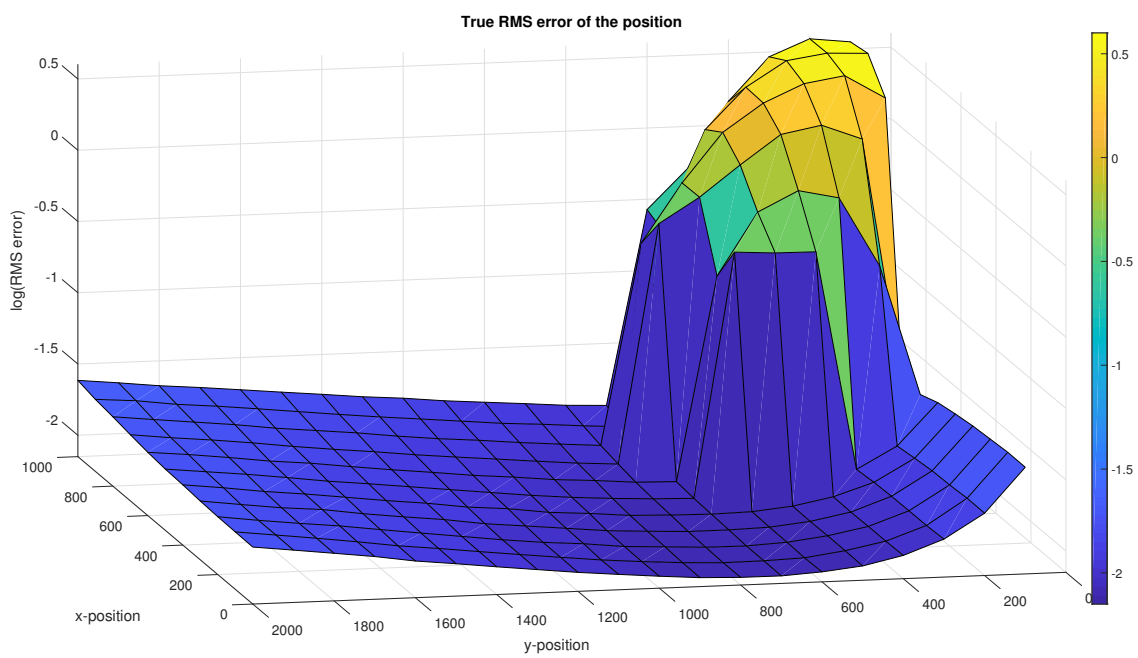

Figure 4.24: The true RMS error on a logarithmic scale of the estimated position found through 10000 Monte-Carlo simulations with carrier frequency of 900 MHz, antenna spacing of 32λ, 64 antennas, transmitter SNR of 15 dB, beacon SNR of 40 dB, antenna array 1 position (-1000,0), antenna array 2 position (1000,0), antenna array 1 tilt $\pi/4$ and antenna array 2 tilt $-\pi/4$

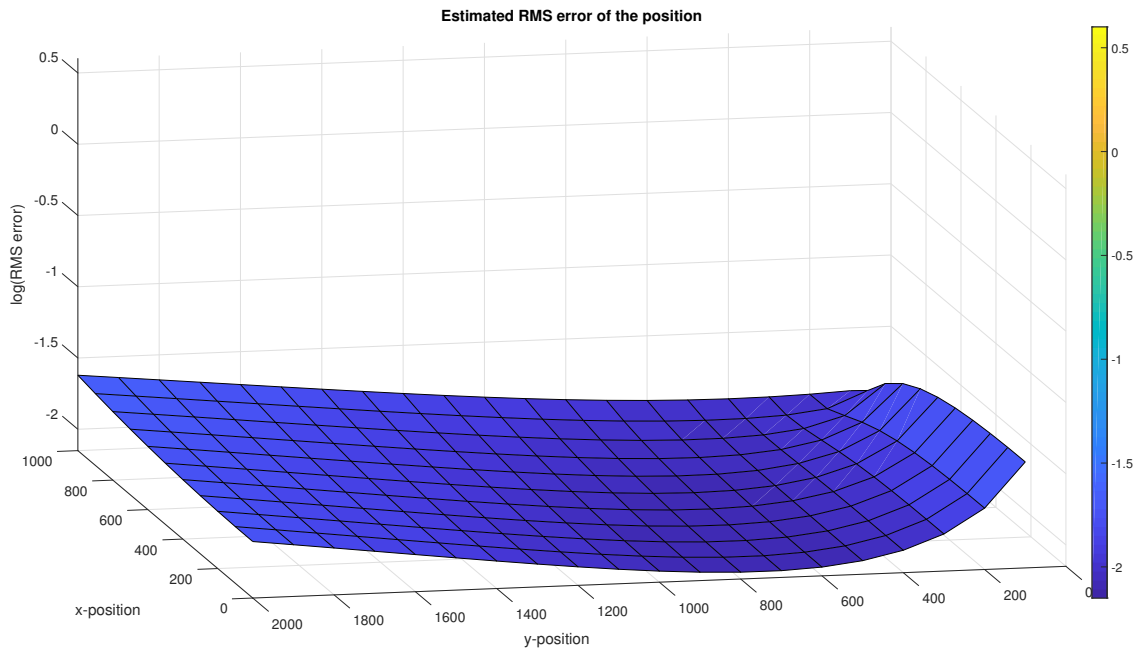

Figure 4.25: The estimated RMS error on a logarithmic scale of the estimated position found through 10000 Monte-Carlo simulations with carrier frequency of 900 MHz, antenna spacing of 32λ, 64 antennas, transmitter SNR of 15 dB, beacon SNR of 40 dB, antenna array 1 position (-1000,0), antenna array 2 position (1000,0), antenna array 1 tilt $\pi/4$ and antenna array 2 tilt $-\pi/4$

Chapter 5

Discussion

5.1 Summary and discussion of the results

The results of all the simulations show that the algorithm gives an estimate of the position with a varying precision depending on different factors, and in this section all the different simulation results will be discussed

5.1.1 Simulation for different positions

The first simulation with tilted antenna arrays and a constant SNR at all positions show the contours of how the system behaves and that as expected the higher the angle the higher the error you get. The estimated error shows the same behavior as the true error even though it is slightly wrong in most positions and the plot of the percentage difference between the two show that this lies in the area of up to 2.6% for the values and positions simulated. For the simulation that used the free-space model for the SNR gave the same exact behavior, but as expected with a larger error caused by the lower SNR in most positions. The estimated error showed the same behavior and in this case, the maximum percentage difference between the two was slightly larger up to 3.9%. The difference between the true and estimated error also shows that for the positions with higher SNR then the constant SNR scenario displays a more precise estimate of the error, and positions with lower SNR give a worse estimate of the error. This indicates that the estimated error is more precise for higher SNRs, which makes sense considering all the linear approximations that were done. When the exact values are compared with the limit found in Figure 4.3 and 4.4 the results show that the system is close to the lower bound and that the estimated error is in fact exactly at the lower bound.

For the simulations that were done using the non-tilted arrays, the behavior remained mostly the same, but in this case, there were higher angles, in the tested area, since the arrays were no longer tilted. The position with the best estimate was still the same (0,1000), although with a higher error. The estimated error did again display the same behavior and the difference between the true and the estimated errors were slightly larger up to 3.3%. This higher difference is probably caused by the fact that higher angles give the same results as lower SNR and the estimated error seems to be worse for lower SNRs. For the simulations using the free-space model the same exact behavior as in the tilted scenario occurred, with the closer positions giving a smaller difference between the estimated and true error and the maximum difference increasing slightly up to 4.6%. When the exact values are compared with the limit found in Figure 4.5 and 4.6 the results show that the flat configuration also is close to the lower bound.

5.1.2 Simulation using different signal strengths

These simulations were done to see how the estimated standard deviations behaved versus the true standard deviation. First, this was done using the same values as the first simulation and by only changing the beacon SNR and it showed that the difference between the two changed depending on the beacon SNR, in Figure 4.20. The results showed that when the beacon SNR was larger than the transmitter SNR, the curve starts to

flatten out and approach the lower limit and that the estimate breaks down at -2 dB beacon SNR. The next simulations in Figure 4.21 show the same figure only this time with multiple curves for different transmitter SNRs. For all the curves the estimated standard deviation flattens out and reach the lower limit when the beacon SNR is equal the transmitter SNR, The true standard deviation, however, flattens out and approach the lower limit at a few decibel higher beacon SNR, around 15-20 dB higher its within 1%, which fits well with the prediction from Section 4.2.

The heatmap in Figure 4.22 display the same simulations and show that for certain beacon SNRs and transmitter SNRs the algorithm falls apart with a drastic increase in the true standard deviation (up to several 100 for low SNRs), which happens at around -2 dB for both signal and beacon SNR. And Figure 4.23 shows that the estimated standard deviation does not show this behavior. This means that if the beacon SNR or transmitter SNR is below this -2 dB value it will not help increasing the other SNR. The requirement for the system SNR will, therefore, be given by this value. Figure 4.7, which shows the difference between the estimated and true standard deviation of the phase rotation ψ, line up with the increase in error for the position and could be the reason it increases so drastically. This increased difference in error is then most likely a combination of all the linear, Gaussian and high SNR approximations that were done.

5.1.3 Effects of spatial folding

The last of the simulations was a system with an even larger distance between the antennas. Figure 4.24 show the true values for the error, it is clear that some of the positions close to either of the antenna arrays show a much larger error, which is not present in the estimated error in Figure 4.24. This is because of spatial folding, which is more present with a larger distance between antennas, as explained previously the system assumes that one picks the correct position and therefore does not take errors caused by this into account. However, if the system has a configuration where this problem is present, it would be as simple as introducing a Q-function using the prior given by correlation and the distances to the closest points from spatial folding.

5.2 Future research

The simulations show good results, but as explained previously there are some factors that limit the algorithm and could be investigated further.

First off the precision of the estimated error at low SNRs is something that could be looked into further. There are a few things in the algorithm that could be the cause of this error, choosing the wrong unwrapped phase, choosing the wrong spatial fold and also the high SNR linear approximations in the factor graph. As mentioned in Section 4.2 it should be possible to do some sort of prediction for when the Gaussian approximation does not hold anymore, and it would be interesting to implement this in the algorithm. Exactly the same can be done for the spatial folding problems since the prior distribution is given, one can just use a Q-function to find the probability of choosing wrong. For the linear approximations in the factor graph, it would be more difficult since for low SNRs the functions can no longer be assumed linear which means the Gaussian approximation does not hold anymore as well. One could possibly look at the second derivative in the Taylor expansion to see if that could be used as an error for the approximation that could be taken into account when calculating the messages.

In the system and the algorithm described there has been one beacon and one transmitter. It should be possible to expand the algorithm for more than one transmitter, assuming that there is used some sort of spreading code and in that case adding a transmitter should only add some noise to the other transmitters depending on the spreading code length. With more transmitters, all of them could be used together with the beacon improving the estimation of the random phase rotation. It might also be possible to not have a beacon at all and just use the transmitters, this would, however, require at least two transmitters to function at all, which might not be desirable in an actual system.

The algorithm here is described using two antenna arrays and both being a ULA. It would be of interest to see if the algorithm could be expanded to include more then two antenna arrays, which would complicate

the calculation of position from AoA and create loops in the factor graph. To not use ULAs would also be interesting since a non-uniform spatial sampling might reduce the problems caused by spatial folding.

Lastly, the system here assumes a stationary target and if the target were to move one would need to reestimate everything, a model where the target could be moving would then be desirable and should be possible with a similar system. As mentioned in Section 2.2.2 the random phase at each antenna drifts over time and one would need to re-estimate the random phase rotation ϕ when the drift is too large. One could, however, include a drifting phase model in the factor graph, where the prior distribution of the phase is depending on the last estimate as well as the model for phase drifting.

Chapter 6

Conclusion

This project aimed to find an algorithm for estimating the unknown position of a transmitter, that is better than simple correlation-based methods, through cloud radio and collaboration in a massive MIMO system. An algorithm based on factor graphs were found. The numerical results showed that the estimated position had an expected value of the true position. The uncertainty of the estimated position approached the lower bound, as long as the beacon SNR was higher than the transmitter SNR and the transmitter SNR was high enough (> 5 dB). The algorithm also estimated the uncertainty of its own estimate and this estimated uncertainty was very precise for high SNRs ($<1\%$ error for 15 dB transmitter SNR and 30-35 dB beacon SNR, figure 4.20), but deviated more and more for lower SNRs. It was also shown that for either beacon or transmitter SNR under -2 dB the system had a drastic increase in uncertainty, which was not predicted by the estimated uncertainty, this then gives the lower limit on the SNR for the system to function properly. Spatial folding problems did occur, but were limited to a few scenarios when the distance between the antennas was large (32λ) and the transmitter was at positions close to the antenna array. These scenarios were not taken into account for the estimated uncertainty and the estimated uncertainty was, therefore, wrong in these scenarios.

In conclusion, this project found an algorithm for estimating the position of a transmitter and simulations showed that was achieved, and that under certain conditions the uncertainty of the estimate approached the lower bound. The algorithm also estimated this uncertainty of the estimated position, that under certain conditions gave a precise estimate of the true simulated uncertainty.

Bibliography

[1] A. H. Sayed, A. Tarighat, and N. Khajehnouri, "Network-based wireless location: challenges faced in developing techniques for accurate wireless location information," *IEEE Signal Processing Magazine*, vol. 22, pp. 24–40, July 2005.

[2] H. Krim and M. Viberg, "Two decades of array signal processing research: the parametric approach," *IEEE Signal Processing Magazine*, vol. 13, pp. 67–94, July 1996.

[3] E. G. Larsson, O. Edfors, F. Tufvesson, and T. L. Marzetta, "Massive mimo for next generation wireless systems," *IEEE Communications Magazine*, vol. 52, pp. 186–195, February 2014.

[4] COST Action CA15104, IRACON, T. Pedersen, and B. Fleury, "Whitepaper on new localization methods for 5g wireless systems and the internet-of-things," 2018.

[5] E. Björnson, L. Sanguinetti, H. Wymeersch, J. Hoydis, and T. L. Marzetta, "Massive MIMO is a Reality - What is Next? Five Promising Research Directions for Antenna Arrays," *arXiv e-prints*, p. arXiv:1902.07678, Feb 2019.

[6] N. Garcia, H. Wymeersch, E. G. Larsson, A. M. Haimovich, and M. Coulon, "Direct localization for massive mimo," *IEEE Transactions on Signal Processing*, vol. 65, pp. 2475–2487, May 2017.

[7] M. Gavish and A. J. Weiss, "Performance analysis of bearing-only target location algorithms," *IEEE Transactions on Aerospace and Electronic Systems*, vol. 28, pp. 817–828, July 1992.

[8] L. M. Kaplan, , and N. Molnar, "Maximum likelihood methods for bearings-only target localization," in *2001 IEEE International Conference on Acoustics, Speech, and Signal Processing. Proceedings (Cat. No.01CH37221)*, vol. 5, pp. 3001–3004 vol.5, May 2001.

[9] K. Doğançay, "Passive emitter localization using weighted instrumental variables," *Signal Processing*, vol. 84, pp. 487–497, 03 2004.

[10] A. Guerra, F. Guidi, and D. Dardari, "Position and orientation error bound for wideband massive antenna arrays," in *2015 IEEE International Conference on Communication Workshop (ICCW)*, pp. 853–858, June 2015.

[11] J. Li and P. Stoica, *Concepts and Applications of a MIMO Radar System with Widely Separated Antennas*. IEEE, 2009.

[12] B. J. Frey, F. R. Kschischang, H. andrea Loeliger, and N. Wiberg, "Factor graphs and algorithms," in *Proc. 35th Allerton Conf. on Communications, Control, and Computing, (Allerton*, pp. 666–680, 1998.

[13] F. R. Kschischang, B. J. Frey, and H. . Loeliger, "Factor graphs and the sum-product algorithm," *IEEE Transactions on Information Theory*, vol. 47, pp. 498–519, Feb 2001.

[14] J. Pearl, *Probabilistic Reasoning in Intelligent Systems: Networks of Plausible Inference*. San Francisco, CA, USA: Morgan Kaufmann Publishers Inc., 1988.

[15] Y. Weiss and W. T. Freeman, "Correctness of belief propagation in gaussian graphical models of arbitrary topology," *Neural Computation*, vol. 13, pp. 2173–2200, Oct 2001.

[16] B. Çakmak, O. Winther, and B. H. Fleury, "S-amp: Approximate message passing for general matrix ensembles," in *2014 IEEE Information Theory Workshop (ITW 2014)*, pp. 192–196, Nov 2014.

[17] S. Rangan, "Generalized approximate message passing for estimation with random linear mixing," in *2011 IEEE International Symposium on Information Theory Proceedings*, pp. 2168–2172, July 2011.

[18] B. Çakmak, D. N. Urup, F. Meyer, T. Pedersen, B. H. Fleury, and F. Hlawatsch, "Cooperative localization for mobile networks: A distributed belief propagation–mean field message passing algorithm," *IEEE Signal Processing Letters*, vol. 23, pp. 828–832, June 2016.

[19] D. Tse and P. Viswanath, *Fundamentals of Wireless Communication.* New York, NY, USA: Cambridge University Press, 2005.

[20] E. Björnson, M. Matthaiou, and M. Debbah, "Massive mimo systems with hardware-constrained base stations," in *2014 IEEE International Conference on Acoustics, Speech and Signal Processing (ICASSP)*, pp. 3142–3146, May 2014.

[21] A. Pitarokoilis, S. K. Mohammed, and E. G. Larsson, "Uplink performance of time-reversal mrc in massive mimo systems subject to phase noise," *IEEE Transactions on Wireless Communications*, vol. 14, pp. 711–723, Feb 2015.

[22] A. Pitarokoilis, S. K. Mohammed, and E. G. Larsson, "Effect of oscillator phase noise on uplink performance of large mu-mimo systems," in *2012 50th Annual Allerton Conference on Communication, Control, and Computing (Allerton)*, pp. 1190–1197, Oct 2012.

[23] S. M. Kay, *Fundamentals of Statistical Signal Processing: Estimation Theory.* Upper Saddle River, NJ, USA: Prentice-Hall, Inc., 1st ed., 1993.

Appendix A

Cramer-Rao lower bound calculations

For starting we have the signal:

$$\boldsymbol{r}[n] = b \cdot \boldsymbol{a} \cdot s[n] + \boldsymbol{w}[n]$$

Where b is the unknown attenuation. Looking at a snapshot at a certain sample of n:

$$\boldsymbol{r} = b \cdot \boldsymbol{a} \cdot s + \boldsymbol{w}$$

Where $\boldsymbol{r}$, $\boldsymbol{a}$ and $\boldsymbol{w}$ is vectors going over the receiver antennas.

$$\mathbf{a} = \exp\left(j2\pi\frac{d_0}{\lambda} + j2\pi\frac{\sin(\theta)\cdot d_{rx}}{\lambda}\cdot m\right) \text{ for } m = 0, 1, ..., N-1$$

Using only the real values:

$$\boldsymbol{r} = C \cdot \cos(2\pi\psi m + \beta) + \boldsymbol{w}$$

Where $\psi = \frac{\sin(\theta)\cdot d_{rx}}{\lambda}$ is the spatial frequency for the change over the antennas, $\beta = 2\pi\frac{d_0}{\lambda}$ and $C = Real\{b \cdot s\}$. So here C, ψ and β are the unknown which we put in the vector $\boldsymbol{\xi}$.

$$\boldsymbol{\xi} = [C, \psi, \beta]^T \tag{A.1}$$

Using the formula for the Fischer information matrix given by:

$$[\boldsymbol{I}(\boldsymbol{\xi})]_{ij} = \frac{1}{\sigma_n^2}\sum_{m=0}^{N-1}\frac{\partial s[n;\boldsymbol{\xi}]}{\partial \xi_i}\frac{\partial s[n;\boldsymbol{\xi}]}{\partial \xi_j} \tag{A.2}$$

Using this with

$$\frac{\partial \boldsymbol{r}}{\partial C} = \cos(2\pi\psi m + \beta)$$

$$\frac{\partial \boldsymbol{r}}{\partial \psi} = -C2\pi m\sin(2\pi\psi m + \beta)$$

$$\frac{\partial \boldsymbol{r}}{\partial \beta} = -C\sin(2\pi\psi m + \beta)$$

The information matrix is then given by

$$[\boldsymbol{I}(\boldsymbol{\xi})]_{11} = \frac{1}{\sigma_n^2}\sum_{m=0}^{N-1}\cos^2(2\pi\psi m + \beta) = \frac{1}{2\sigma_n^2}\sum_{m=0}^{N-1}(1 + \cos(4\pi\psi m + 2\beta))) = \frac{N}{2\sigma_n^2}$$

$$[\boldsymbol{I}(\boldsymbol{\xi})]_{12} = -\frac{1}{\sigma_n^2}\sum_{m=0}^{N-1} C2\pi m\cos(2\pi\psi m+\beta)\sin(2\pi\psi m+\beta) = -\frac{C\pi}{2\sigma_n^2}\sum_{m=0}^{N-1} ms \in (4\pi\psi m+2\beta))) = 0$$

$$[\boldsymbol{I}(\boldsymbol{\xi})]_{13} = -\frac{1}{\sigma_n^2}\sum_{m=0}^{N-1} C\cos(2\pi\psi m+\beta)\sin(2\pi\psi m+\beta) = 0$$

$$[\boldsymbol{I}(\boldsymbol{\theta})]_{22} = \frac{1}{\sigma_n^2}\sum_{m=0}^{N-1} C^2(2\pi m)^2\sin^2(2\pi\psi m+\beta) = \frac{(C2\pi)^2}{2\sigma_n^2}\sum_{m=0}^{N-1} m^2(1+\cos(4\pi\psi m+2\beta)$$

$$= \frac{(C2\pi)^2}{2\sigma_n^2}\sum_{m=0}^{N-1} m^2 = \frac{(C2\pi)^2}{2\sigma_n^2}\frac{2N^3-3N^2+N}{6}$$

$$[\boldsymbol{I}(\boldsymbol{\xi})]_{23} = \frac{1}{\sigma_n^2}\sum_{m=0}^{N-1} C^2 2\pi m\sin^2(2\pi\psi m+\beta) = \frac{\pi C^2}{\sigma_n^2}\sum_{m=0}^{N-1} m = \frac{\pi C^2}{\sigma_n^2}\frac{(N-1)N}{2}$$

$$[\boldsymbol{I}(\boldsymbol{\xi})]_{33} = \frac{1}{\sigma_n^2}\sum_{m=0}^{N-1} C^2\sin^2(2\pi\psi m+\beta) = \frac{NC^2}{2\sigma_n^2}$$

Here we have used the two approximations below that hold as long as ψ is not close to 0 or $\frac{1}{2}$. This is the case when the incident angle is not close to $0°$ or $\pm 90°$.

$$\sum_{m=0}^{N-1} n^i\sin(4\pi\psi m+2\beta) \approx 0$$

$$\sum_{m=0}^{N-1} n^i\cos(4\pi\psi m+2\beta) \approx 0$$

Which gives the matrix

$$\boldsymbol{I}(\boldsymbol{\xi}) = \frac{1}{\sigma_n^2}\begin{bmatrix} N/2 & 0 & 0 \\ 0 & 2C^2\pi^2(\frac{2N^3-3N^2+N}{6}) & C^2\pi\frac{(N-1)N}{2} \\ 0 & C^2\pi\frac{(N-1)N}{2} & \frac{NC^2}{2} \end{bmatrix}$$

The CRLB is given as the inverse of the information matrix, which is given by

$$\boldsymbol{I}(\boldsymbol{\xi})^{-1} = \begin{bmatrix} 2\sigma_n^2/N & 0 & 0 \\ 0 & \frac{12}{(2\pi)^2\cdot SNR\cdot N(N^2-1)} & \frac{6(N-1)}{SNR\pi(N^3-N)} \\ 0 & \frac{6(N-1)}{SNR\pi(N^3-N)} & \frac{2(2N-1)}{SNR\cdot N(N+1)} \end{bmatrix}$$

Where the signal to noise ratio SNR is given by

$$SNR = \frac{C^2}{2\sigma_n^2} \tag{A.3}$$

The CRLB for an estimate for ψ is then given by

$$var(\hat{\psi}) \geq [\boldsymbol{I}(\boldsymbol{\xi})^{-1}]_{22} = \frac{12}{(2\pi)^2\cdot SNR\cdot N(N^2-1)} \tag{A.4}$$

And the CRLB for an estimate of β is

$$var(\hat{\beta}) \geq [\boldsymbol{I}(\boldsymbol{\xi})^{-1}]_{33} = \frac{2(2N-1)}{SNR\cdot N(N+1)} \tag{A.5}$$

This then gives a lower bound for the estimation of ψ and β, to get a lower bound for the estimation of the incident angle θ and the distance d_0 we use

$$\boldsymbol{g}(\boldsymbol{\xi}) = [C, \theta, d_0]^T = [C, \arcsin\left(\frac{\psi\lambda}{d_{rx}}\right), \beta\frac{\lambda}{2\pi}]^T$$

The Jacobian of this matrix is then given by

$$\frac{\partial \boldsymbol{g}(\boldsymbol{\xi})}{\partial \boldsymbol{\xi}} = \begin{bmatrix} 1 & 0 & 0 \\ 0 & \frac{\frac{\lambda}{d_{rx}}}{\sqrt{1-(\psi\frac{\lambda}{d_{rx}})^2}} & 0 \\ 0 & 0 & \frac{\lambda}{2\pi} \end{bmatrix}$$

$$\frac{\partial \boldsymbol{g}(\boldsymbol{\xi})}{\partial \boldsymbol{\xi}} = \begin{bmatrix} 1 & 0 & 0 \\ 0 & \frac{\lambda}{d_{rx}cos(\theta)} & 0 \\ 0 & 0 & \frac{\lambda}{2\pi} \end{bmatrix}$$

The CRLB for an estimate of θ is then given by

$$var(\hat{\theta}) \geq [\frac{\partial \boldsymbol{g}(\boldsymbol{\xi})}{\partial \boldsymbol{\xi}}]^2_{22}[\boldsymbol{I}(\boldsymbol{\xi})^{-1}]_{22} = \frac{12}{(2\pi)^2 \cdot SNR \cdot N(N^2-1)} \frac{\lambda^2}{d_{rx}^2 \cos^2(\theta)} \tag{A.6}$$

And the CRLB for an estimate of d_0 is

$$var(\hat{d}_0) \geq [\frac{\partial \boldsymbol{g}(\boldsymbol{\xi})}{\partial \boldsymbol{\xi}}]^2_{33}[\boldsymbol{I}(\boldsymbol{\xi})^{-1}]_{33} = \frac{2(2N-1)}{SNR \cdot N(N+1)} \cdot \frac{\lambda}{2\pi} \tag{A.7}$$

For a complex signal the CRLB is then given by

$$var(\hat{\theta}) \geq \frac{6}{(2\pi)^2 \cdot SNR \cdot N(N^2-1)} \frac{\lambda^2}{d_{rx}^2 \cos^2(\theta)} \tag{A.8}$$

$$var(\hat{d}_0) \geq \frac{(2N-1)}{SNR \cdot N(N+1)} \cdot \frac{\lambda}{2\pi} \tag{A.9}$$

NTNU

Kunnskap for en bedre verden